Faculty of Agricultural and Environmental Sciences
Department of Bioresource Engineering
BREE 495 – Design 3

Multistage Greenhouse Acclimatization System

Submitted by:

Guillaume Cere

Adam Nunez

Maxime Nectoux

Ervin Cai

Advisor: Dr. Mark Lesfrud

Professor: Dr. Chandra Madramootoo

April 14, 2021

Abstract

In horticulture, it is common practice to start high value crops from either seeds or cuttings inside a nursery greenhouse environment to promote growth and resilience (Arteca, 2015). Once growth has reached a certain extent, these crops are transplanted outside, where climatic conditions are harsher and less stable. Consequently, it is well known by farmers that if plants are transplanted too rapidly from an indoor to an outdoor environment without proper acclimatization, most crops will be stressed and will lose vigour, resulting in lower yields (Stoneham.J and all, 1985). In collaboration with a cannabis growing start-up company, CanaCanna Corp, the objective of this design project is to determine and model the most efficient system to acclimatize high value crops that are grown in a greenhouse environment and transplanted outside for flowering. Multiple models exploring the possibilities to acclimate plant cuttings were discussed and analysed. Based on user friendliness, materials, operating costs, capacity to mimic outside conditions, safety, durability, and an innovative greenhouse roll-up system allowing the independent opening and closing of different greenhouse sections was designed. To ensure user-friendliness, an automation component controlled by a GUI was also implemented. Furthermore, to ensure the feasibility and sustainability of the project, preliminary analyses were conducted to examine the economic, social, and environmental aspects of the design. Finally, an add-on design allowing the automated opening and closing of 6 independent sections to be implemented on a standard 102’ x 30’ gothic greenhouse was conceived. Moreover, a scaled down prototype was constructed and confirmed the conceptual feasibility of the design. However, due to time and budgetary constraints, the downward motion of the mechanism did not function as designed.

Keywords: Plant acclimatization, Greenhouse systems, Roll-up sides, Automation, Plant nursery

List of Acronyms and Abbreviations

CAD	Computer Aided Design
DC	Direct Current
AC	Alternating Current
DIY	Do It Yourself
GUI	Graphical User Interface
IoT	Internet of Things
M-V-C	Model-View-Controller
PGR	Plant Growth Regulators
RPM	Revolutions per Minute
SoC	System on a Chip
SPF	Sustainability Projects Funds
UX	User Experience

1. Introduction

With global increases in population and consumption, the demand for horticultural high-value crops is steadily increasing worldwide. Agricultural lands being limited, a frequently tackled solution to solve the crop demand problem is to focus on reducing crop losses both in the field and in the post-harvest operations (FAO, 2019). Another approach that is currently gaining interest in the world of crop engineering and agronomic research is to design both the crops and their environment to maximize yields produced by each individual plant. In horticulture crop production it is well documented that it is economically beneficial to propagate plants either from seeds, cuttings, or in-vitro culture in a controlled greenhouse environment (Wang et al.,2007). The young plants are therefore grown up to a desired size in an environment where humidity, temperature, lighting, and wind are controlled to favor optimal plant growth (Xin and Tong, 1986; Wang et al., 2007). The plants are then sold to be transplanted outside either by individuals or agricultural corporations. Because of the drastic and rapid environmental change imposed to the plants, a phenomenon known as transplant shock often happens at this stage resulting in plant damages, increased insect and diseases vulnerability, retarded growth or even plant death, all of which causing important yield losses.(Stoneham et al, 1985) Indeed, if not well prepared, transplants can be broken down by an increase in wind, burnt by the drastic increase in solar radiations or shocked by the temperature change and the new soil environment. To tackle this problem, many different systems of plant hardening/conditioning have been imagined and put in place by researchers and farmers to produce suitable transplants that are ready to be transplanted (Philo, 2012). Common visual indicators of a healthy well-suited transplant are that it is short and stocky with thick, strong stems and deep green color (Latimer and Beverly, 1993).

Many different acclimatization processes such as in vitro, plant growth regulators (PGR) and mechanical conditioning approaches exist in the literature. (Teixeira da Silva, 2007; Hazarika, 2003) This being said, farmers all have their own way of acclimatizing their transplants. After on-site visits and research, it was concluded that a common approach to this problem is to gradually move the plants from inside the greenhouse to an outdoor environment for some hours and take them back inside after (Philo, 2012). This process must be done multiple times to obtain satisfactory results and growers need to ensure that outside conditions are appropriate (moderate winds, no rain and moderate solar radiance) (Philo, 2012). This process can be labour intensive and costly when running large operations. While looking online, no commercial processes or apparatus are currently suitable to perform such a task. It is therefore with that purpose in mind that, with the support of Dr. Mark Lefsrud, associate professor at McGill University and CanaCanna Corp, a cannabis growing company, our team aims to design a stress reducing multistage greenhouse acclimatization system that is adaptable to various high value crops and produce ready to transplant crops from unrooted cuttings. After thorough discussions and literature reviews made in the previous report, this report focuses on the feasibility of a system allowing greenhouses to open their sides at a desired height in order to allow users to control inside environmental conditions and progressively expose plants to outside conditions. In order to test the feasibility of such a system, a small-scale prototype was built and analysed. A discussion on the implementation potential of such a system was also elaborated.

Vision Statement: *Improve acclimatizing process for outdoor transplant of high value agricultural products.*

2. Needs statement and Target Specifications

In the previous semester, the team discussed and identified essential needs and important specifications that led to the design proposed in this paper. An overview of the final needs and their respective description follows:

Outside conditions mimicry (-): To prepare the plants to be transplanted outside with as little stress as possible, the plants need to be exposed, in the weeks before transplant, to a progressive shift from the greenhouse conditions to the outside world conditions. The system will therefore need to be able to provide a way to gradually reproduce the outside environmental conditions as precisely and holistically as possible. Environmental conditions to be considered will be temperature, relative humidity, wind speed and light intensity and composition.

User friendliness (+): It was very important for the client to have a system that is easy to use by the workforce. In countries like Laos or Mexico, workers operating in agricultural systems might not have high educational background. Therefore, access.

Safety (+): The design should comply with safety standards and promote worker's health and safety. Strategies should be undertaken to prevent risks of failure that could lead to any damage. Duration of greenhouse opening, and closing should also be kept under a minute.

Durability (-): The design should be sturdy, with minimal maintenance and adequate material life span.

Costs (+) Relatively low cost materials are preferred, with particular attention to the sub-costs for installation, operation and maintenance.

Consequences of the COVID-19 pandemic, such as material shortage and inflation as well as changes in the manufacturing industry protocols were solid obstacles and this greatly influenced the team decisions for the directions to take on the conception of the design prototype. In addition, this greatly delayed the operation plan of CanaCana Corp in Laos. Therefore, the team decided to redirect the project and put more emphasis (+) on a low cost and safe device, taking the durability and outdoor conditions mimicry to a lower extent (-). This means that the prototype will show that the opening and closing mechanism work, without promising the best durability and effective mimicry of the outdoor conditions through its running. A more concise description of the prototype Design Specifications is explained in the next sections.

3. Literature Review

3.1 Plant Acclimatization

Over time, three main branches of plant conditioning have been developed. The first only applies to in-vitro propagated plants in which plant tissue cells are exposed to specific chemicals before even being a plant, this process shapes the future seedling in a specific predetermined way to respond better to a specific outside condition such as high soil salinity, high temperature, etc.(Hazarika ,2003) The second one is done by using plant growth regulators (PGRs) to modify the plant structure by applying different hormones or hormone inhibits to the growing plant.(Teixeira da Silva, J.A. 2007) This method has the potential of modifying the plant's height, internodal spacings, increasing branching and removing excess fruits (Omafra, 2020). The last method is known as mechanical conditioning, this method is performed by subjecting the plant to external forces in order to provoke a growth response. (Latimer and Beverly, 1993) Common conditioning techniques include rubbing stems, brushing shoots, shaking potted plants and whole flats, vibrating pots or plants, and perturbing plants with water, forced air, or wind (Latimer and Beverly, 1993). All of these operations can either be done manually or simply by putting the plant in the appropriate environmental setting so that it is subjected to the desired forces.

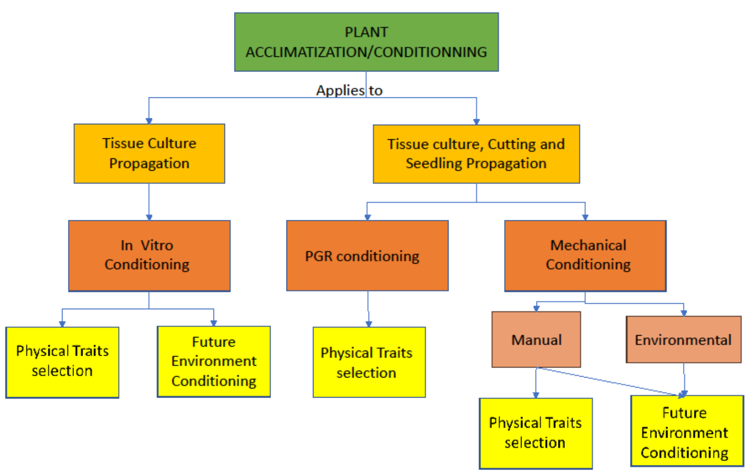

Fig.1: Plant Acclimatization techniques and applications

3.2 Roller Shutters and Curtains

The basic principle of such systems is explained in fig. X: a door/curtain (14) material is secured at its end to a cylindrical roller (16) which is rotated in a first direction to lower the door and in a second, opposite direction to retract the door. The curtains can be made of one uniform material or of multiple panels. A cylindrical roller is mounted above the doorway and is rotationally displaced by an electric motor and drive assembly (24, 26) via a drive shaft (19). It also requires the presence of two vertically aligned, parallel side track frames (32, 34) facing lateral edges of an opening (12). Materials for the curtains can be light and transparent. It is usually high strength plastic material such as polyvinyl chloride (PVC). A rapidly displaced overhead roll type door with good insulating material is particularly desirable for energy savings in greenhouse applications, especially when a large differential occurs between inside and outside temperatures.

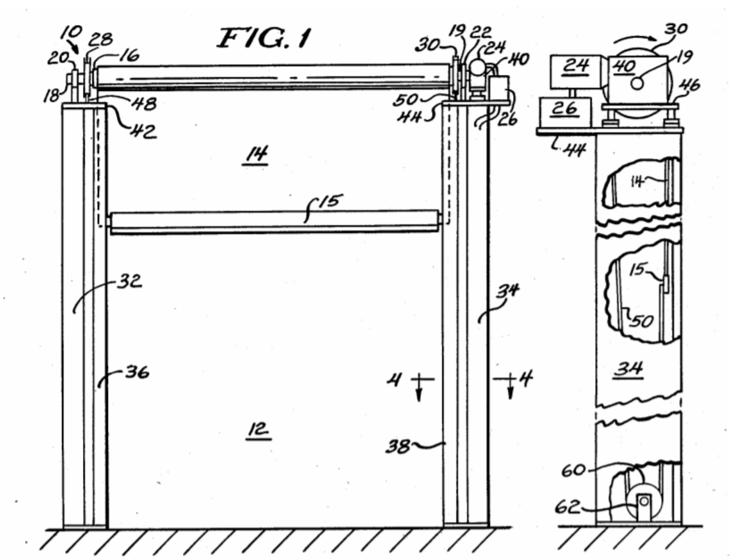

Fig.2: *Front view of roll-up door system (left) ; Partially cut-away side view of roll-up door system right) (Kraus, 1989). Patent Number: US4887660A*

Note that the lower end extremity of the curtain has a bottom rail (15). This permits protection of the curtain's lower end from impacts and gives relative rigidity to the curtain once closed. One mounting bracket (20,22), secured to a panel (42,44) on the upper end of each of the side frames is designed to provide support and allow free rotation of the cylindrical roller.

Considering the electrical system: a motor, controller (24,26) and a gear box (40) coupled to a drive shaft (19) are also mounted on one of the panels on one side of the cylindrical roller. A non-driven support shaft (18) is placed on the opposite side. A pulley (28,30) with belt (48,50) is attached to each shaft. The second end of each of these belts is attached to the bottom rail (15) of the curtain. The door is thus able to roll up or down from the tube while being maintained in a stretched condition under tension. A lower pulley (60) is mounted in the lower portion of each of the side frames with a belt wound around to ensure continuous applied tension.

3.2.1. Ulti Group Full Vision Doors

The product described relates about the work of the company Ulti Group and their transparent PVC roll-up doors.

Fig.3: Ulti Group transparent PVC roll-up doors (Ulti Group Ltd, 2018)

The dimensions of the roll-up door are 6 meters width and 7-meter height (Ulti Group Ltd, 2018). The door opening Speed is stated at 1.5 m/s and the system can resist wind speeds reaching up to 140km/h (Ulti Group Ltd, 2018). In figure 3 we can see that the PVC roll is sequenced with red stripes that must be made of a more rigid material. A roll bar is also present up the door from which we can see the rotation initiating the movement of the "curtain". On the sides, we can see two opposing metallic structures that should be guide tracks/channels through which the PVC slides through. The PVC roll movement in the guide tracks is led by a metallic layer/bar and a rubber material that enable better insertion of the curtain in the guide tracks.

3.2.2 Garage door

As an automated roll up system requires a dynamic opening/closing mechanism to be attached to the arched greenhouse, it is necessary to review mechanisms with curved tracks/rails. A mechanism for opening and closing a garage door made of several panels is described in the next section and relates to the invention of Karl Stoltenberg from 2004.

With respect to figure 10, we can see inner horizontal tracks (16) radiused downwards at point 18 and connected with an inner pair of vertical tracks (14) to form a continuous track. The support movement guidance of the garage door is ensured by an outer pair of vertical tracks (12) attached adjacent to the inner vertical tracks. Other points of interest here are the guide members (22) and the panels sliding through it, forming the door. This component includes rollers (24) or equivalent that extend laterally out from the sides of the door to the vertical tracks (14). These rollers are embodied with shafts (26) and bearing (27) englobed in extension brackets (30), each attached to the inner surface of the door (31). Shaft journals (28) are parts of the upper panel brackets and permit opening/closing of the door. Note that the shaft journals at the lowermost panel (29) are mounted on the sides (36) on the lower inner surface of the garage door. This placement allows the rollers (24) to engage the inner vertical section of tracks (12) while the door is either open or closed. A pulley (40) is set on the ground, adjacent to the bottom of the inner vertical tracks.

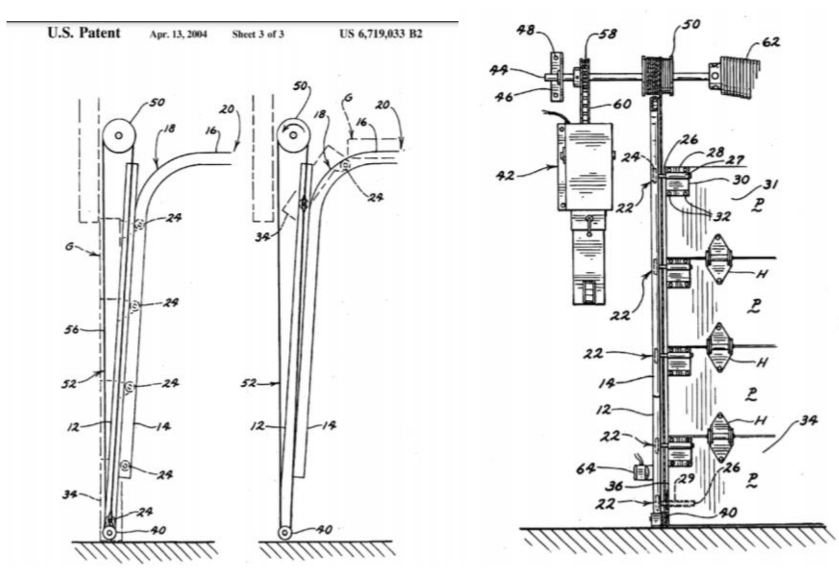

*Fig.4: Power operated multi-paneled garage door opening system (*Stoltenberg, 2004). *US6719033B2*

Considering the electrical and mechanical components, a flexible cabling system (52) is located on each side of the door. The cables are fit onto drums and around the pulley.The lift cable sections (54) are attached to the lowermost shaft journals (29) and bear the load of the door when lifted. Each reverse cable (56) then wounds around the bottom pulley. This configuration ensures that the lift and reverse cables move simultaneously, maintaining a constant tension in the flexible cabling system which provides a safety feedback mechanism in case any obstruction is encountered. A torsion bar (44) is present on the wall horizontally above the garage door and fixed with brackets (46). A motion sensor (64) can be used to detect any motion under the door while closing/opening. Opening of the door is accomplished by actuating a Jackshaft operator which initiates rotation of the torsion in the clockwise direction (Stoltenberg, 2004). The jack shaft is drivingly connected to the torsion bar by a chain (60) and sprocket (58). At least one torsion spring (62) on the torsion bar permits counterbalancing of the weight of the door as it is being lifted. Closing of the door is accomplished by actuation of the Jackshaft operator causing the torsion bar to rotate in the counterclockwise direction.

The actions of the pulleys and the support frames enable the door to be maintained tensile in any position, similar to the roller shutters. Using motion sensors for safety is also a valuable method that could be used at the commercial scale.

3.3 Motor

This section will cover two Direct Current (DC) motors commonly used for actuation in industrial automation applications.

3.3.1 Stepper Motors

Stepper motors are brushless, synchronous DC motors whose rotor rotates in specified angular increments. Contrary to regular DC motors, stepper motors have a stator that is composed of individual sets of coils. The coils are paired to form an electromagnet and energised using a driver (see figure 13). When the coils are energised in sequence, they rotate the motor in steps in order to complete a rotation. (Acarnley, 2002)

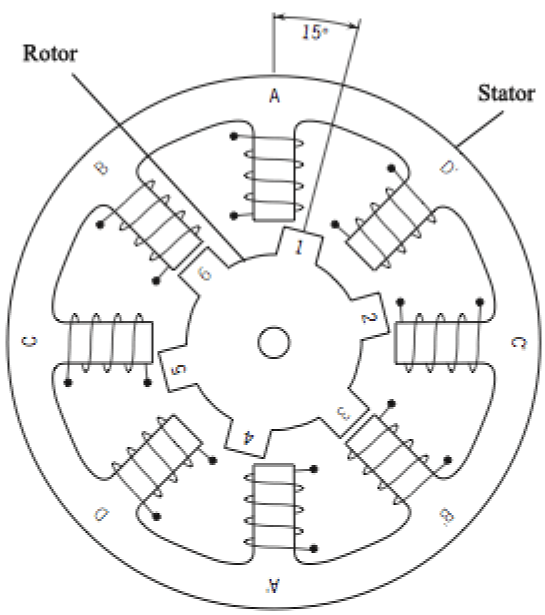

Figure 5: Rotor-Stator disposition of a stepper motor (Aswinth, 2018)

There exist three main types of stepper motors, distinguished by their construction layout. Firstly, variable reluctance motors have an iron core which is magnetically attracted to the stator poles. Moreover, Permanent magnet motors have a permanent magnet rotor which is directly attracted or repelled by the stator depending on the applied pulses. And lastly, Hybrid synchronous motors constitute an amalgamation of both aforementioned motors (ElProCus, 2020). Additionally, based on the type of stator winding used, stepper motors can be classified as either unipolar or bipolar. In the former, the motor operates with one winding containing a center tap per phase. In contrast, bipolar driven motors only contain a single winding per phase. The stepper motor is used in various industrial applications where torque at low speed, high-speed dynamic and positioning accuracy are considered essential. For instance, applications of the stepper motor include but are not limited to roll bending, wrapping machines, drilling and extrusion machines and 3-D printers (Kenjo and Sugawara, 2003). Moreover, a stepper motor's position can be accurately controlled without any feedback sensors, and therefore makes it ideal for applications in automation and robotics (Gay, 2014).

3.3.2 Gear Box

Epicyclic gear trains, often referred to as planetary gears, are composed of four different elements capable of various speed rations all within a compact layout (Lewis, 1984). These elements include:

1) Sun Gear: externally toothed ring gear, coaxial with the gear train
2) Annulus: internally toothed ring gear, coaxial with the gear train
3) Planets: externally toothed gears, mesh with the sun gear and annulus
4) Planet Carrier: support structure for the planets, coaxial with the gear train

Due to the compact form factor, epicyclic gear trains have a considerable advantage over parallel shaft gears in terms of reductions in weight and space. These advantages are derived from the various components within the gear trains and the interactions between the components. The use of multiple planets allows for loads to be distributed across multiple tooth contacts in addition to the coaxial arrangement providing a more compact layout.

3.5 Automation

Accelerating developments in embedded systems, Internet of Things (IOT), and cloud computing systems have made automation attainable at low costs. Embedded systems are often defined as a processor-based system design for dedicated functions and are built around microcontrollers (Forrai 2013). Being designed for specific tasks, they are often optimized for space, production costs, performance, and reliability. Conventional automation systems for commercial and industrial use often require long research periods, experimentation, and testing; in addition to those drawbacks, conventional automation systems are often custom made for specific situations and are rigid in terms of implementation. A simple embedded system is ideal for sites with a rapidly evolving environment or projects with pricing constraints. Do-it-yourself (DIY) platforms like Arduino and Raspberry Pi based systems are a suitable alternative to conventional solutions for building embedded systems compatible with greenhouses. The implementation of these systems supply flexibility, low power consumption and are easy to manage (Türk et al 2015). Automation can even have significance in areas with cheap labor; developing nations often lack the resources to hire highly specialized individuals with the expertise to operate these large growing operations. Automation has been seen by many as a viable alternative for skilled knowledge-based workers whose jobs involve data-driven decision-making (Henry-Nickie, 2017). An automated process will reduce uncertainty within operations in addition to the ability to operate outside of standard working hours which is preferred by many growers who apply acclimatization treatments during non-working hours (J. Latimer & B.Beverley, 1993).

3.5.1 Microcontrollers and Compact Computers

The hardware components of DIY embedded systems often revolve around a combination of both the Arduino Uno and Raspberry Pi. The Arduino uno is a microcontroller capable of reading and writing digital and analog values; specifically, the Uno is capable of listening for, processing, and displaying information (Arduino, 2019). The raspberry pi 4B is a compact computer with an arm-based system on a chip (SoC) ideal for embedded systems programmed for specific tasks (Raspberry Pi, 2020).

3.5.2 Model-View-Controller Architecture

A simple yet effective software design pattern is essential to implementing a functional graphical user interface. The Model-View-Controller (M-V-C) approach (Fig. 18) details an architecture design that separates the back-end logic from the front-end graphical presentation (Nor et al., 2018). The Model-View-Controller separates the system into three main components. The model is the logical unit of the domain, consisting of classes which model and manage the data, logic, and parameters of the application. The view is the component which presents the information and logic, consisting of classes which give a visual interface to the application. The final component, the controller, will accept inputs from the user and convert them into commands for either the Model or View. Using the M-V-C approach for designing an automated system will allow for a rapid development process. The User Interface (View) can be readily replaced or updated without impacting the backend logic of the Model.

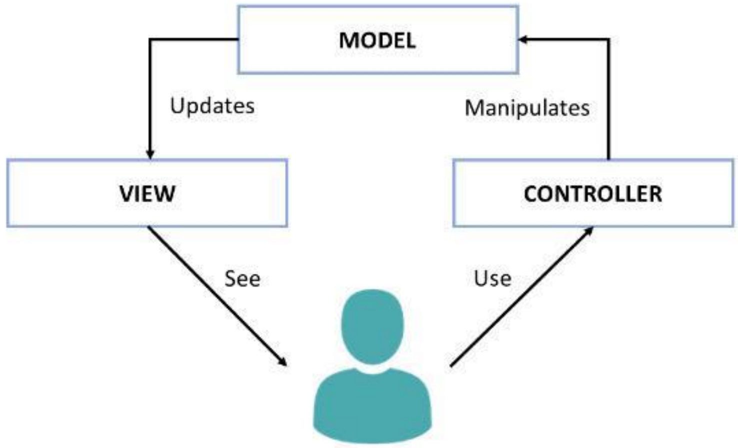

Fig.6: Model-View-Controller User Interactions. Source: Nor et al., 2018

A finite-state machine will need to be implemented in conjunction with persistence and object streams. This allows for the M-V-C architecture to output values which are not only dependent on the input but also the history of past events (saves past data).

3.5.3 Graphical User Interface

When designing the graphical user interface (GUI) for the view component of the M-V-C architecture, various ergonomics principles for software design should be followed. Emphasis should be put on both visuals and user experience (UX), taking into account both the location and type of user who will be interacting with the display. Another key principle that should be emphasised is the avoidance of reverse engineering the mapping of a mouse pointer to the user interface touch locations (Sonkar, 2019). Therefore, large text boxes and buttons should be designed to provide ease of use along with clear graphics indicating the current state of the system. Affordance, or the cues which give hints as to how the user may interact with a specific component of the use was also taken into consideration.

4. Final Design Components

4.1. Structural layout

The final modeled design includes six independent mechanized roll-up systems, integrated into one standard 102x 30 ft horticultural greenhouse frame structure (see fig.7 below). A gothic style arched greenhouse was chosen as it offers better climatic control and is adapted to resist high winds. They are also fitted to the Mexican and US climatic regions. The team has designed the system and additional components for this structure shape. It should be made in galvanised steel which is a strong and corrosion resistant material making it reliable and affordable for a greenhouse structure that is exposed to outside conditions. Sections 1 through 4 are 36 x 15 ft, whereas sections 5 and 6 are 30x 15 ft. The sections include a roll-up bar that facilitates the curtain opening/closing on each side of the greenhouse. One curtain is therefore required per section. Each plastic curtain will be divided by 6 bars of aluminum that will be engaged in the C-channel framing of the same material thanks to a roller mechanism. These bars permit the curtain to stay tight and be engaged in the C-channels, they also give the envelope more resistance to wind as further discussed in the Embedded Bars" Section. The bars will be extended by a roller mechanism at their ends. The channels will be fixed to the arches on each side of each section of the greenhouse. The channels should therefore follow the same geometry. The curtain will be able to span over the tracks thanks to the roller mechanism consisting of polyurethane overhead door rollers (McMaster-Carr, 2020). The mechanism should be able to self-lock and unlock when desired.

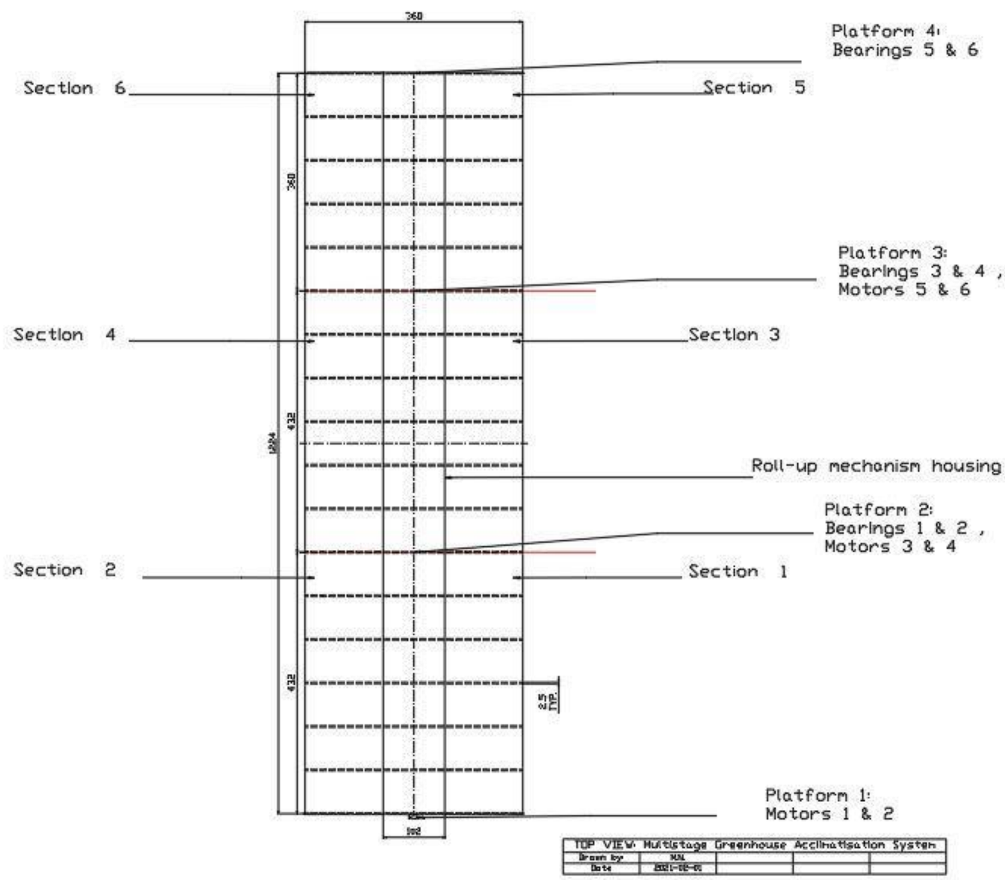

Fig 7: Multistage Greenhouse Acclimatisation System Structural Layout Top View

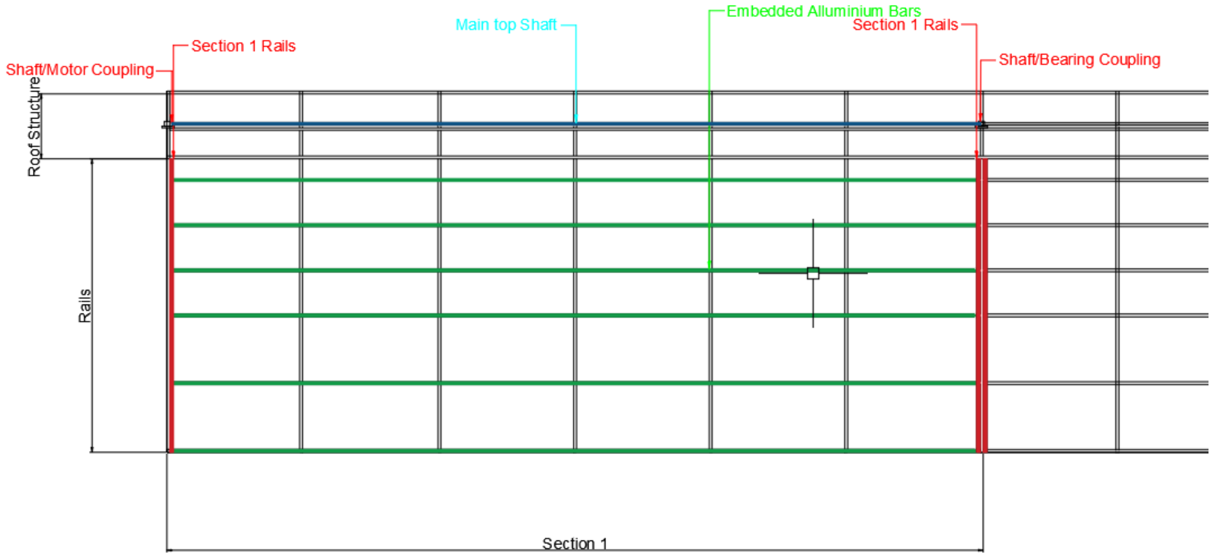

Fig 8: Multistage Greenhouse Acclimatisation System Structural Layout Side View of Section 1

4.2. Motor/shafts housing design

The housing component spans two feet and is 1 foot high at the ridge beam (fig 9). It was designed specifically to protects the roll-up mechanisms from foreign material and rain, as well as covering the space created between the two roll up mechanisms. Thus, a dome layout as seen in Figure 9 was chosen for these purposes. To make sure that the dome would be aerodynamic and would not cause structural problems, the height had to be minimized efficiently, to do so, the following calculations were done to estimate the required space to house the plastic roll. For the same reasons as the ones stated above, this structure will also be built with galvanised steel. The structure would then be covered using a single layer of polyethylene which would be anchored by wire locks. With a 1/16” wall thickness, a width of and thickness of 1.5”, the weight of the specific components of the housing add-on can be calculated for further structural analysis.

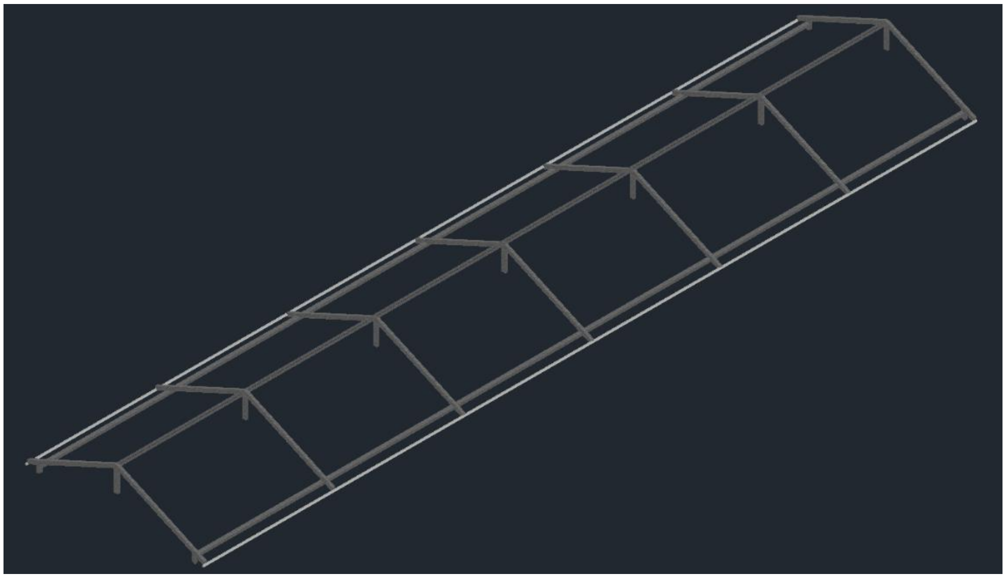

Fig 9: Motor/Shaft housing structural design for Section 1

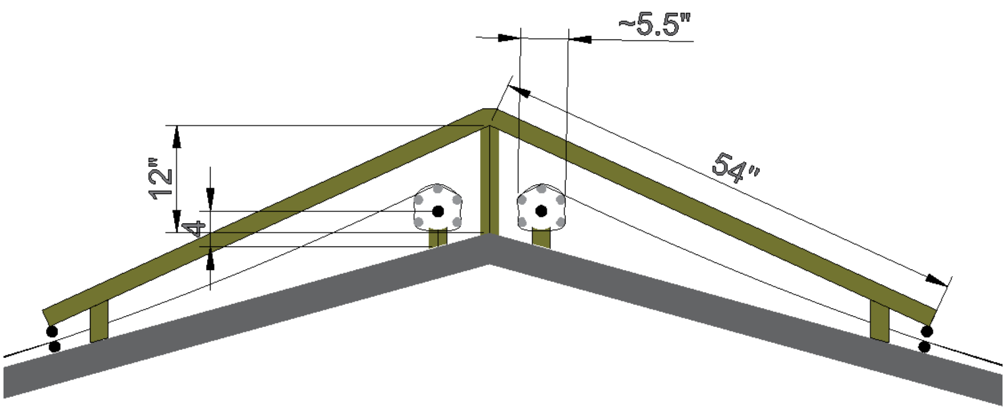

Fig 10: Motor/Shaft housing 2D front view with dimensions.

Optimum Height Calculations

To calculate the roll radius, the following equation was used.

$$R = \sqrt{}(L \times t/\pi + r2)$$

Where r is the shaft radius, t is the plastic thickness and L is the plastic length.

$$r = 1" = 2.54cm$$

$$t = 8\,mil = 0.0204cm * 2(double\ plastic): 0.0408\ cm$$

$$L = 300\, in = 762\, cm$$

So, if the plastic is tightly rolled on the shaft, the radius of our roll is going to be 3.2”. Adding to that the diameter of one of the 1” rods passing through the plastic that will also be rolled around the shaft and we get a value of 5.2”. Therefore, to account for discrepancies, we assumed that the roll will be around 5.5” as shown on the model below. Accounting for this, the roll ups should be elevated from the roof structure by 4” and we chose to make the total dome height of 1’ to allow maintenance access and proper airflow. Moreover, to ensure an aerodynamic profile we wanted to make sure that the angle created on the roof was not too steep, so we made the roof sides 54” inches long. All these parameters have been tried and rectified to also make the model eye-pleasing.

Properties of galvanized steel roof extension structure: (using ASTM A-36 steel)

- density: $0.00803\ g/mm^3$
- Area of beam cross section :1.5 x 4 x 0.0625” = $0.375\ in^2$

or 38.1*4* 1.537mm = $242\ mm^2$

- Total length of beams on full structure: 1224*3 + 54 * 36 + 4* 18 + 3*36 = 5724 in (145389.6 mm)
- Total volume: 242 mm^2* 145389.6mm = 3519500 mm^3
- Total weight: 70369000 * 0.00803 g/ mm^3 = 282550g or 282. 55kg

The total weight added by the housing structure to the greenhouse is therefore 282.55 kg

Covering Material

The covering material used in the commercial scale application would be based on the suggested industry standards, the American Standards, and the Mexican Standards. The plastic chosen for this project is therefore standard UV II treated double layer 8mil polyethylene. It is indeed important to have UV II treated plastic to ensure a long-lasting life for the material. As the inner layer is not directly exposed to UV II rays it does not need to be UV II treated to avoid condensation on the inner walls of the greenhouse, polyethylene retailers propose a drip-treatment that repels water from condensation on the plastic layer. (Harnois 2017). It was therefore chosen to include that anti-condensation option to make our design up to standards. As the total greenhouse dimensions are 50ft x 102ft to allow proper installation, bigger dimensions are required to be bought. Plastic rolls of 55ft x 108ft were suggested by Harnois specialists. This therefore makes a total plastic aera of 5940 ft^2 per layer for a total of 11 880 ft^2 (1103.7 m^2) for the two layers. However, on average, PE film only lasts about 3-4 years.

Properties of Low-Density PE cover

- Use of double layer polyethylene film
- Thickness of 0.2 mm (i.e. ~ 8 mil) per layer
- Density of Low-Density Polyethylene (LDPE): 0.920 g/ cm^3= 920 kg/m^3

Area covered for one section on one side and volume:

$$A = \left[\left(\frac{432}{2}\right) * \ 25\right] ft^2 \quad * \ (0.3048^2 \ m^2) \ = \ 77.42 \ m^2$$

$$V = \ A * t = \ 77.42 \ * \ 0.0004 \ = \ 0.031 \ m^3 \qquad\qquad (double\ layer)$$

Total mass of plastic

$$mp\ (section) \ = \ 920 * 0.031 \ = \ 28.52 \ kg$$

$$mp = \ \rho * v * number\ of\ sections \ = \ 920 * 0.031 * 6 \ = \ 171.12 \ kg$$

Embedded bars

To hold the plastic in place and ensure its tightness we needed to add metal bars that would go lengthwise and be connected to rollers on its extremities. This bar is a central piece to the design as its size and weight is going to affect other components such as the motor size. It is also important to take into consideration that the polyethylene plastic will not be able to resist high tension, so the bar weight needs to be light enough to ensure plastic viability. An iterative process to choose the best bars possible to serve our purposes was therefore made. After review of the possible alternatives, Aluminum hollow steel bars will be used for the commercial scale. These bars of 1 ¼" diameter have a wall thickness of 1/16". To embed these bars in the double layer polyethylene plastic, a special thermal treatment will need to be applied to the plastic to fuse the two plastic layers together and create a pocket in which the bars could be pushed. As the prototype suggested, a total of 3 embedded bars for a midsize structure was sufficient, it was therefore estimated that a total of 6 bars would be required for the full-scale prototype. As the longest section of the greenhouse is 432", the weight of one bar is 5.7 lbs for a total of 34.2 lbs for 6 bars. Those bars will be evenly distributed along the greenhouse's side as seen in figure 20. As there are 6 sections, 36 bars will be required, representing a weight of 205.2 lbs (93.32kg).

Rails and structural brackets

To adapt the system to the greenhouse, custom made zinc coated galvanized steel rails will be required. After an analysis of the different possibilities available on the market, it was determined that the best option was to make precise drawings of the required rails and send the design to a garage door manufacturing facility. The rails indeed need to be carefully bent and adapted to the greenhouse's structure. As seen in figure I of the appendix IV, the C channel shaped rails shall be able to welcome 2" diameter rollers.

Track

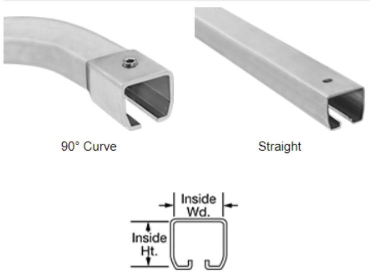

Lg.	Track Radius, ft.	Inside Wd.	Inside Ht.	Thick.	Material	Color	Mounting Fasteners Included	Mounting Hole Dia.		Each
100-lb. Track Capacity										
90° Curve										
3' 2"	2	1 3/8"	1 1/8"	0.06"	Galvanized Steel	__	No	3/8"	1040A28	$115.74
Straight										
8'	__	1 3/8"	1 1/8"	0.06"	Galvanized Steel	__	No	3/8"	1040A21	52.61
10'	__	1 3/8"	1 1/8"	0.06"	Galvanized Steel	__	No	3/8"	1040A22	65.20
600-lb. Track Capacity										
90° Curve										
3' 2"	2	1 3/4"	2 5/16"	0.19"	Powder-Coated Steel	Tan	No	9/16"	1862A27	242.69
4' 9"	3	1 3/4"	2 5/16"	0.19"	Powder-Coated Steel	Tan	No	9/16"	1862A28	277.25
6' 3"	4	1 3/4"	2 5/16"	0.19"	Powder-Coated Steel	Tan	No	9/16"	1862A29	295.28
Straight										
10'	__	1 3/4"	2 5/16"	0.19"	Powder-Coated Steel	Tan	No	__	1862A26	128.46

Fig.11 Representation of C-channel and Box-channel geometry and nomenclature (Johnson Bros. Metal Forming Co)

As determined on the prototype, the rails are not required on the full length of the arch. Indeed, the rails will stop at the beginning of the motor/shaft housing. Therefore, knowing that the total greenhouse arch is 25' and the roofing goes up to 54" from the top of the greenhouse, the required rails will have a total length of 20'6". The required tracks for this design should be able to resist a moving load of at least 400 lbs (bars + plastic), the 600 lbs capacity tracks proposed by McMaster Carr are therefore good options for this design.

The custom rails should therefore have the following characteristics and be bent on the same path as the greenhouse's arch.

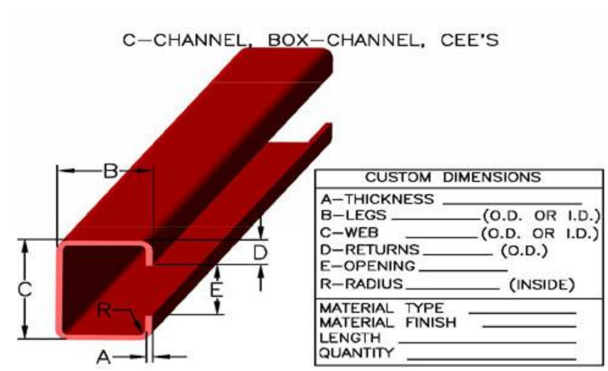

Fig.11 Representation of C-channel and Box-channel geometry and nomenclature (Johnson Bros. Metal Forming Co)

Data	C-channel dimensions (SI units) - mm	C-channel dimensions (empirical units) - inch.
Web Inner Diameter	40.31	1.902
Web Outer Diameter	50.75	2
Leg Inner Diameter	35.61	1.402
Leg Outer Diameter	38.05	1.498
Returns	16.64	0.655
Opening	17.48	0.688
Metal Thickness	1.22	0.048

Table 1: Dimensions of the C-channels required for the project (Johnson Bros. Metal Forming Co)

Zinc Galvanised steel rails properties: (metric)

- Length: 20.5' → 6.24m → 6240mm
- Thickness: 1.22 mm
- Total width: C + 2*B+2*D = 160.2 mm
- Volume: 121960 mm^3
- Density: 0.000803 g/ mm^3
- Weight of rail: 9793g

So the total weight of each individual track is around 10 kg, which will be distributed evenly on the arch at a rate of 1.57g/mm.

Furthermore, for better structural performances, as proposed by standard greenhouse building practices, the fixation of the tracks on the arches will be reinforced with **support bracket**s. They are needed for every 5 ft. (1.524m) of 600-lb. capacity track (McMaster-Carr, 2020). Therefore, 5 support brackets will be required for each rail section. The support bracket should be fitted for a 50.75 x 38.05 mm = 1.93 *10^{-3} m^2 inner area rails. The dimensions of the support brackets will be such that they allow complete fixation of the rails to the arch. The cross-sectional area of an arch being 2.5'' x 1.5''. Individual support bracket weights will be assumed to be 1kg. The total associated load is 1kg*5*6 = 30 kg

Wheels

The 2" rollers used in the protype construction were standard garage door rollers. Such wheels would also be adapted for the full-scale prototype. A custom adaptor could be inserted into the stem of the roller inside of the 1 ¼" metal bars going across the greenhouse. The wheels are made of polyurethane, and 12 x 6 = 72 units will be required in total. This corresponds to a total weight of 350.64g x 6 = 2103.84 g

4.3 Platform design

Platforms are required to safely fix the shaft-motor assembly to the greenhouse structure underneath the mechanism housing. The platforms are 24x22 in and made of galvanized steel. Moreover, they are directly bolted to both the arches and the ridge beam and reinforced with steel trusses for maximum stability (see fig 12. below). As described in the structural layout, the platforms contain either motors, bearings, or both for mirrored and/or adjacent sections. The platforms span two feet on a dual slope under the housing, with a flat central section bolted to the ridge beam. Extra space on the platforms was provided for electronic components, ease of access for maintenance purposes, and added stability.

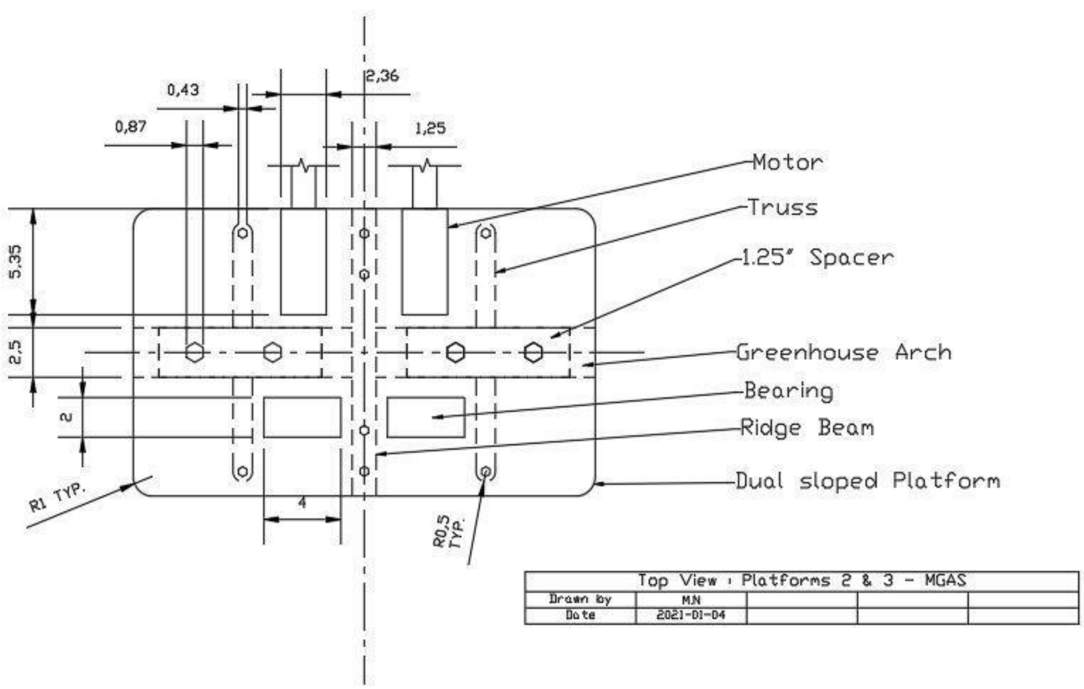

Fig 12: Top view of platforms 2 and 3

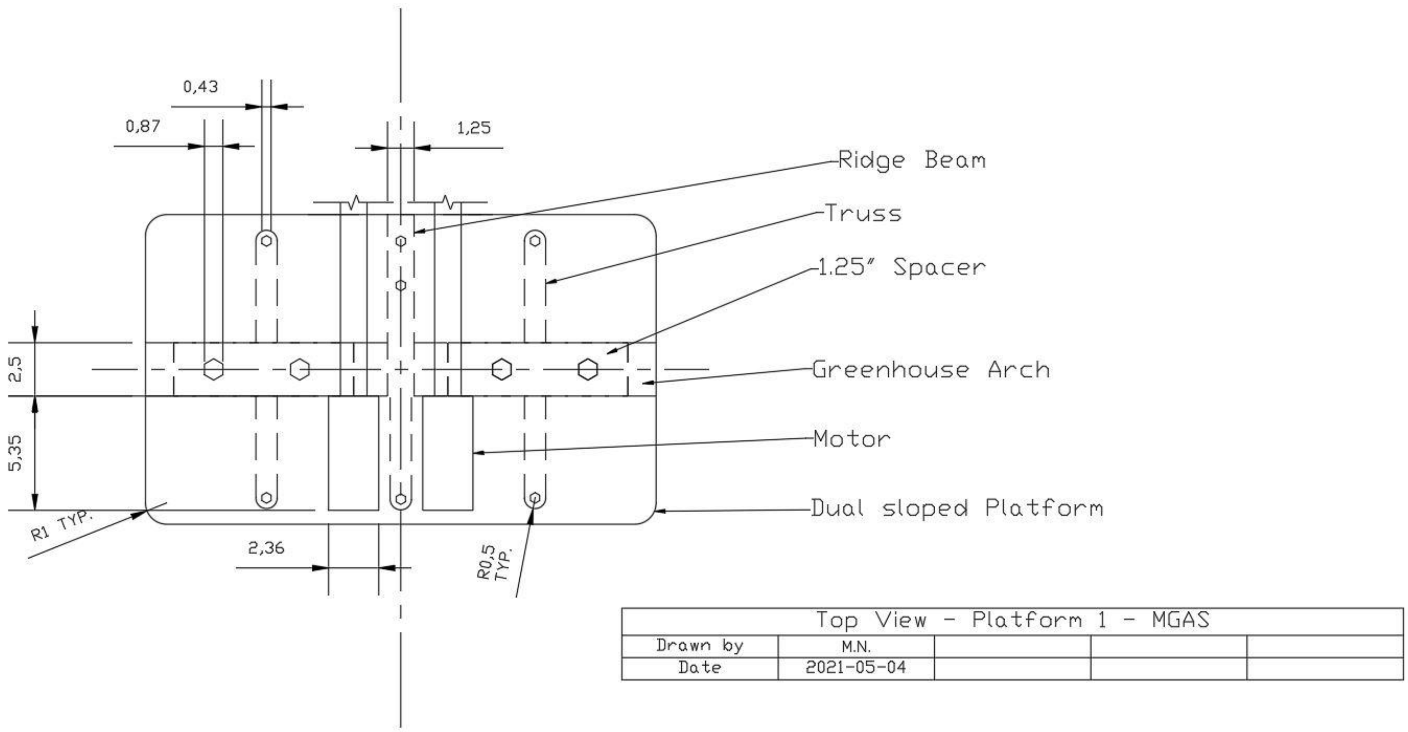

Fig 13: Top view of platform 1

Platform 4 is identically fixed to the structure as platform 1. However, the former only contains bearings for shaft 5 and 6.

4.4 Motor assembly

The stepper motor was chosen for its high holding and operating torque capabilities at lower speeds, longer life span and higher durability when compared to conventional dc motors, reliability, and high positional accuracy. To choose an adequately sized motor, an approximate analysis of the various loads and inertia acting on the system as well as the torque developed, motion profile, power requirements was completed as follows.

Motor Properties:

Refer to appendix III, a single motor weighs 1.5 kg. Accounting for 6 motors over the whole greenhouse, this will represent 6 local loads.

Load analysis and motor requirements
Estimated static loading per shaft

Assumptions:

- Use of double layer polyethylene film
- Thickness of 0.2 mm (i.e. ~ 8 mil) per layer
- Density of Low-Density Polyethylene (LDPE): 0.920 g/cm^3 = 920 kg/m^3

Area covered for one section on one side and volume:

$$A = \left[\left(\frac{100}{3}\right) * 25\right] ft^2 * (0.3048^2 m^2) = 77.42\, m^2$$
$$V = A * t = 77.42 * 0.0004 = 0.031\, m^3 \quad - (double\ layer)$$

Total mass of plastic per shaft

$$mp = \rho * v = 920 * 0.031 = 25.4\, kg$$

Mass of horizontal bars embedded in double film plastic:

$$mb = [5.71\, lbs) * 1/\, 2.2\, kg] * 6\, bars = 15.6\, kg$$

Mass of rollers in channels:

From Appendix I,

$$m(roller) = mr = 350.64\, g = 0.351\, kg$$

Total mass suspended on shaft is then:

$$mt = mp + mb + mr = 41.4\, kg$$

Inertial properties, motion profile and torque requirements

Assumptions:

- Simplified load torque model (free hanging, neglecting slope torque)
- Rolling friction in the channels is negligible compared to load.

Total static Load

$$Fs = mt * g = 41.4 * 9.81 = 406.14\, N$$

Load Torque

With a chosen standard shaft diameter of 2in (0.0508m),

$$T = Ft * r = (406.14) * (0.0254) = 10.3 \quad N.m$$

Load to Rotor inertia ratio

Stepper motors have recommended Inertia ratios to ensure adequate operating conditions. The inertia of the load can be calculated using the estimated total static load. Therefore, knowing the load inertia, the rotor inertia can be estimated to fit a recommended Inertia ratio for the motor itself. For our design, we chose an operating inertia ratio of 5:1, as per recommended by various motor manufacturers.

Load inertia

$$J(L) = (mt) * r^2 = (41.4) * (0.0254)^2 \; kg.m^2 = 0.0267 \, kg.m^2$$

Rotor inertia

Applying the desired inertia ratio yields:

$$J(m) = (1/5) J(L) = (1/5)\, 0.0267 = 5.34 * 10^{-3} \; kg.m^2$$

Total inertia

$$J(T) = J(L) + J(m) = 3.20 * 10^{-2} \, kg.m^2$$

Motion profile of the motor

For the motor, the motion profile of the load was defined as a symmetric trapezoidal acceleration and deceleration model (see figure below), typical to brushless stepper motors. As such, a period of acceleration is followed by a period of constant velocity (i.e., run velocity) and then a period of deceleration until the motor stops and applies its holding torque. Indeed, following this motion profile, we can determine acceleration and deceleration values for a chosen run velocity (Vmax), and subsequently determine torque requirements for changes in velocity.

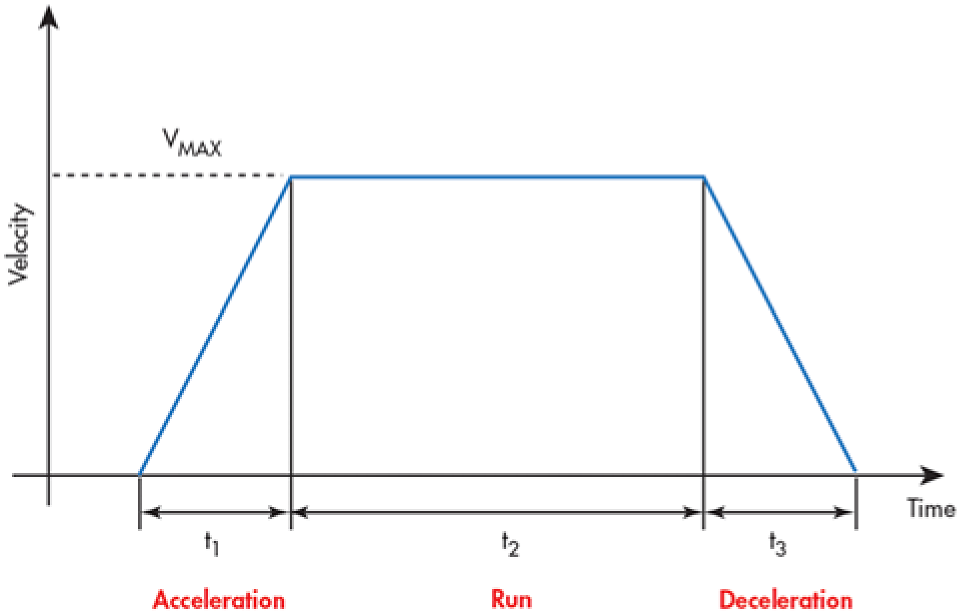

Fig.14: Trapezoidal motion profile (Motion Control & Motor Association,2017)

Chosen operating Velocity

$$\frac{\frac{Total\ path\ length}{(2 * pi * r)}}{(2\ mins)} = 300\ in\ /\ (\ 2 * pi * 1\ in)\ /\ 2mins\ = 23.9\ rpm\ \ \sim \mathbf{25rpm}$$

Therefore, we chose an operational Velocity of 25 rpm to accommodate an opening time of equal to or under 2min for the greenhouse sides, according to the specifications of the customer.

To translate to linear velocity:

$$V = \frac{(2\,pi.r)}{60} * \ rpm$$

$$V = \frac{2\,pi.r}{60} * 25 = \ 6.65\ * \ 10^{-2}\frac{m}{s}$$

Determining acceleration/deceleration time

Just like any motor, a stepper motor requires a certain time to start from speed 0 to reach its stable working speed, this part is denoted as motor acceleration, the same concept applies for deceleration. Allotting 40% of the total motor stepping for both acceleration and deceleration, as used in previous applications for bipolar stepper motors (Quinones, 2012), we can fix the acceleration and deceleration time at 24 seconds each (i.e. 20% of the 120 second operation time).

Resulting acceleration:

$$a = \frac{V}{(t1)} = \frac{6.65 * 10^{-2}}{12} = 2.77 * 10^{-3} \frac{m}{s^2}$$

Resulting deceleration:

$$a = \frac{-V}{(t1)} = -\frac{6.65 * 10^{-2}}{12} = -2.77 * 10^{-3} \frac{m}{s^2}$$

Acceleration Torque:

$$T(acc) = Jt\,(a) + TL = 10.3 \;\; N.m$$

Deceleration Torque:

$$T(dec) = Jt\,(-a) + TL = 10.3\, N.m$$

- For the selected stepper motor, the rated power is 0.0336 kW.

The **running torque** can therefore be expressed as:

$$T = \frac{9550P}{n} = 9550 * \frac{0.0336}{25} = 12.84\, N.m$$

Neglecting idle time, **the RMS torque requirement for the motor** is as follows:

$$TRMS = SQRT\left[\frac{Tacc^2(tacc) + Trun^2(trun) + Tdec^2(tdec)}{tacc + trun + tdec}\right]$$

$$\boldsymbol{Trms = 13.56\, N.m}$$

Safety factor

The chosen stepper motor has a rated torque of 23.54 N.m with a planetary gearbox system and a 76 49/64 :1 gear ratio.

Therefore, we can compute the safety factor as follows:

$$SF = \frac{Rated\ Torque}{Trms} = \frac{23.54}{13.56} = \mathbf{1.74}$$

In fact, an iterative process was pursued by pre-selecting a motor with a rated torque and by determining the torque requirement for our application to ensure the motor can meet the requirement with an adequate safety factor. The rated torque of the chosen motor achieved a safety factor of 1.74, taking into consideration the required RMS torque. Industry leaders in automation recommend safety factors between 1.5 and 2.25 for torque requirement (AMCI, AA, 2020). Therefore, the chosen motor provides adequate torque to comply with industry standard safety factors. See appendix II for the chosen motor specifications.

4.5 Shaft strength analysis

The allowable torsional shear of the shaft material was computed to serve as a basis for comparison with the maximum torsional shear developed in the shaft. Furthermore, torsional deflection of the shaft was evaluated with the load torque. A large safety factor will be deemed acceptable since the torsional strength of the shaft is not considered to be the limiting factor in the strength of the design. Nevertheless, the mechanical analysis will serve to verify the integrity of the chosen shaft, given its material and dimensions.

ASME code recommends the following relationship between allowable shear stress and the ultimate strength of the material:

$$\tau_{all} = 0.18(S_{ut})$$

Our shaft is composed of AISI 1018 Mild carbon steel, with the following properties:
Sut = 440 MPa
E = 205 GPa
G = 80 GPa

Therefore:

$$\tau_{all} = 0.18(440) = 79.2\ MPa$$

Maximum Shear Stress

The maximum shear stress developed in a hollow cylindrical shaft can be computed with:

$$\tau_{max} = \frac{Tr}{J} = \frac{T\left(\frac{D}{2}\right)}{\left[\frac{\pi(D^4 - d^4)}{32}\right]}$$

Using the load Torque and shaft geometry from the previous sections, we obtain:

$$\tau_{max} = \frac{\left[10.3 * \left(\frac{0.0508}{2}\right)\right]}{[\pi(0.05080^4 - 0.04921^4)]} = 3.35\ Mpa$$

We obtain a safety factor with the following equation:

$$\frac{\tau_{all}}{\tau_{max}} = SF$$

Resulting in:

$$\frac{\tau_{all}}{\tau_{max}} = \frac{79.2}{3.35} = 23.6$$

Therefore, the chosen shaft geometry and material complies with safety requirements.

Torsional deflection of the shaft

The angular deflection of the shaft incurred by torsion can be calculated as:

$$\theta = \frac{LT}{JG} = \frac{LT}{\left[\frac{\pi(D^4 - d^4)}{32}\right] G}$$

Resulting in:

$$\theta = \frac{(10.973)(10.3)}{[\pi(0.05080^4 - 0.4921^4)](80\ .10^9)} = 0.181\ rad = 1.04°$$

4.6 Automation and Motorization

The design aims to automate a standard roll up system by utilizing various stepper motors and an array of hardware and software components. The integrated automation system will enable end users to program specific periods throughout the day where the roll up will be activated. Data on the system as well as the surrounding environment will also be made available to the user through our graphical user interface (GUI). Future additions to the automation system could involve the implementation of a sensor network and the use of machine vision to obtain and process larger quantities of data for the user to improve growing operations. Preliminary testing on the feasibility of machine vision in detecting the quality and quantity of crops was conducted utilizing OpenCV in combination with a

Raspberry Pi and Pi Cam. A conclusion was made that the use of machine vision and other sensors was plausible and beneficial for future implementation.

4.5.1 Hardware Design

The implementation of hardware components for greenhouse automation is based around several key electronic and mechanical devices; the connection between components is summarized in Figure 15. An Arduino Uno was crucial in communicating with stepper motors through the microstepper driver. The Arduino Uno is also necessary in reading/writing various input, output, and states of the stepper motors through a serial connection with the main Java controller class. For the full-scale system, multiple Stepper motor drivers will be connected to the Arduino Uno, which will control the six stepper motors required for all motorized sections. The Raspberry Pi is the second major hardware component for our system as it operates as a microcomputer for data transfer with the Arduino system. This allows for a GUI to be displayed on an external touchscreen which is ideally mounted on the inside of the greenhouse beside the entrance. The display will allow for touchscreen interactions which can control basic greenhouse roll up functions and select times for the automation settings. Alternatively, the graphical user interface could be implemented on a removable table device or even though a mobile app. A stylus could also be integrated into the system when touchscreen inputs with the finger are unavailable, such as when gloves are worn.

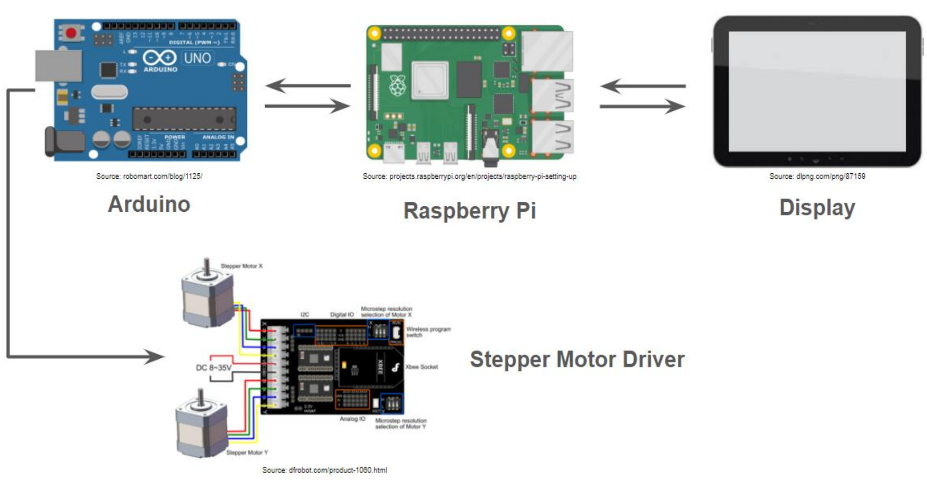

Fig.15 Interaction Between Hardware Components

4.5.2 Software Design

The software components of our design are run on the Raspberry Pi and will be implemented using the MVC architecture. For the model component, Umple was used to create a UML class diagram which produced the adequate skeleton java code[1] required to complete the controller and view. The controller or backend of our system is implemented with mostly Java and Arduino. For the view or front end, multiple languages were required including javaFX, XML, and CSS. All Arduino based code for the automated system will be sent via a serial connection initiated within the Java code from the Raspberry Pi to the Arduino. Any values or states read by the Arduino will also be transmitted back to the Raspberry Pi and displayed on the GUI.

4.5.3 Graphical User Interface

The GUI is designed to have a static menu bar along with a static information panel, this design layout was evaluated as the most suitable solution for a touch-based interface with emphasis on simplicity. The menu bar is situated on the left side of the display and transitions to the various pages which correspond to the specific button. Refer to Figure 16 for the roll up control and automation screen. The addition of blank tabs (home, climate, and settings) has been included for aesthetic purposes and for future implementation. This would be needed for a fully climate-controlled greenhouse with an integrated sensor network. A static top panel will also be utilized to display basic information which can be supplemental to the roll up system, including the company name, the date and time, as well as outdoor conditions.

[1] GitHub Repository Link for Complete Code: https://github.com/BREE490-Engineering-Design/Design-2.git

Figure 16. Graphical User Interface for Roll Up Controls

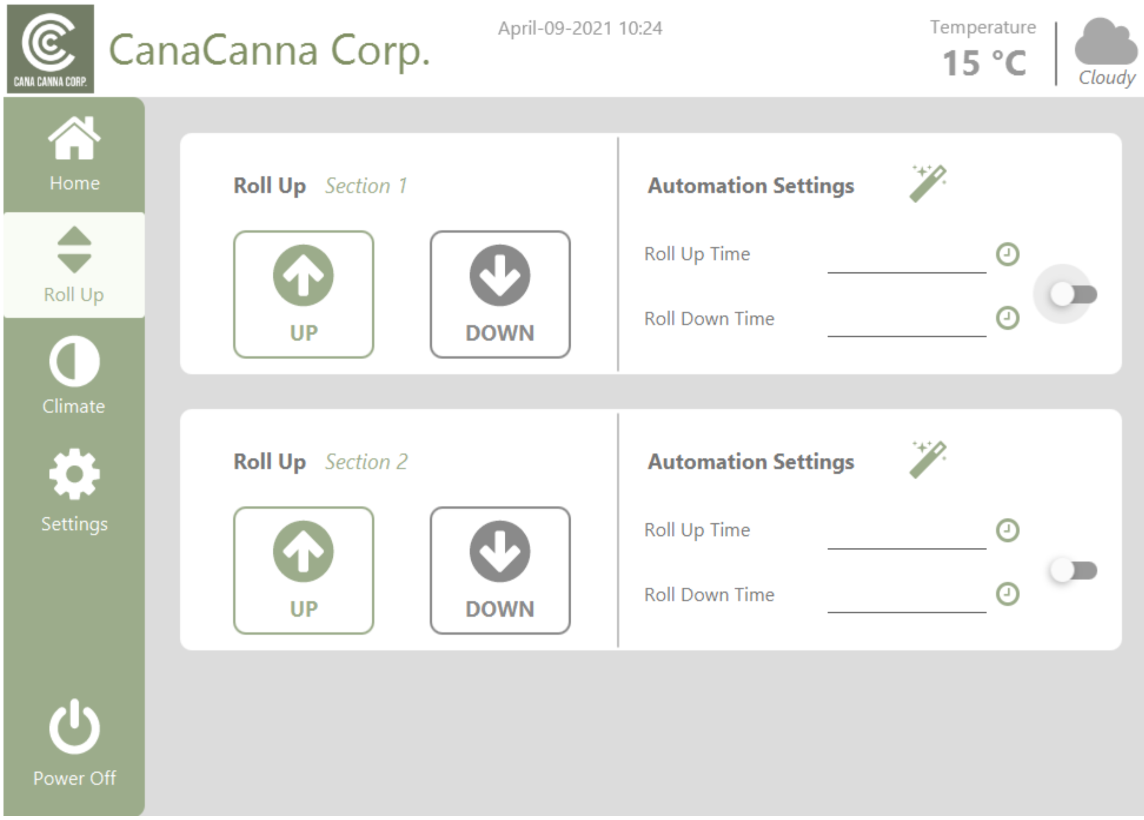

5. Commercial scale design

To adapt the concept to potential future commercial applications, it is important to understand and account for all the important parameters influencing the safety of the user during free-standing greenhouse operations. The team therefore investigated acceptable methods of Design and Construction of Greenhouses. The team identified the American Standard (ANSI A 58.1-1972) from the National Greenhouse Manufacturer Association (NGMA) and the Mexican Standard NMX-E-255-CNCP-2008 (AMCI, 2008). These standards give general information about the minimum different loads that the greenhouse structure should be able to withstand, the satisfying insulation properties of the roof covering materials, rheological behaviours (i.e., for wind) as well as important specifications on the loads acting on the structure. An analysis of the structural and design loads is available in the next sections.

As a preliminary step, US and Mexico weather information was processed to provide concise data to use in the load calculations (i.e., for rain, snow). Forecasts will be used to account for Global Warming in the analysis. General rules for safety diverted from the OSHA regulations are also added to the report

5.1 Structural and Design Analysis

As general requirements, greenhouse structures and all associated parts shall be designed and constructed to safely support all loads, without exceeding the allowable stresses for the materials from which the greenhouse is constructed. The NGMA defines four types of loads:

Dead load: Weight of permanent components of the greenhouse (i.e covering material, roof structure, heaters, water pipeline, all fixed service equipment…)

Live load: Weight due to the use or to rain. A live load is a non-permanent load, it can be furniture that will be displaced, a worker walking on the roof for repairs, or weight due to rain. Note that a live load that "hasn't moved" for 30 days is considered a dead load.

Wind load: Load caused by wind forces from any horizontal direction. They are determined by defining velocity pressures, a gust response factor, and a drag coefficient. When wind blows on a structure, its force creates an overturning moment that must not exceed two-thirds of the dead load stabilizing moment. Otherwise, the greenhouse structure should be anchored. In specific locations, an exposition factor is determined to account for variations of the wind in the area.

Snow load: Based on climatological data. Snow load acting on a greenhouse depends on roof slope, snowfall on the ground and temperature information, snow depth of 7.5 cm (wet) or 30 cm (dry) is equivalent to 2.5 cm depth of water.

In addition, Greenhouse structures and their components shall have adequate stiffness to limit vertical and transverse deflection, vibrations or any other deformation that may adversely affect their structure. Finally, a greenhouse structure should demonstrate general structure integrity, i.e., being able to sustain local damage with the structure and remaining stable.

The determination of these loads and the complementing structural analysis are carried with much more details in the next sections. Load effect on the individual components and connections of greenhouse structures shall also be determined by accepted methods of structural analysis. The following section assesses climatic data in the US and Mexico for temperature, precipitation, snowfall, and wind speeds.

5.1.1 Climate and Weather Information

The team decided to associate the range of applications of such a system to certain climate regions. The team thus targeted implementing the prototype in the southern US and North Mexican climate.

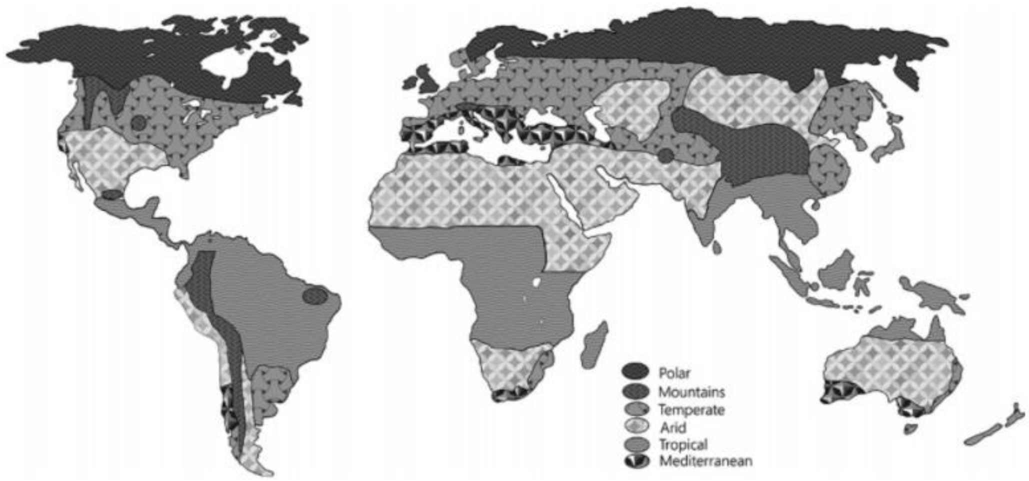

Fig. 17: Agro-climatic Zones in the World (Ponce et. al, 2015)

Referring to fig. 17, the US and Mexican climates are arid and temperate. This permits the team to experiment the mechanism on an arched greenhouse, judged suitable for such climates. Drawings of the arched greenhouse system prototype are available in the next section, after a review of the various materials used for construction.

Temperature is a crucial factor for the greenhouse controlled environmental conditions. It can also influence the choice of cladding material and layout, as well as ventilation system. According to the National Oceanic and Atmospheric Administration, the yearly temperature for North America can be considered in the range 0-110 °F (-18 to 43 °C) for future estimations (Pierce, 2014). In addition, it was reported that global temperature in North America has been increasing at an average rate +0.29°C/decade since 1981 (NOAA, 2021). Due to time restrictions and limited scope, the team didn't perform a heat requirements analysis. It is however a crucial aspect and will need to be determined for further work. Acceptable values for various locations are generally available from state energy offices and organizations such as the American Society of Heating, Refrigeration and Air Conditioning Engineers (ASHRAE, 1978).

Precipitation varies greatly with location. There are also a lot of uncertainties about the natural variability of rainfall events. In addition, the South-East of the US is a zone of high hurricane risks. While a lot of information is available on precipitation, for the purpose of this project it is more relevant to use extreme maximum rainfall data. The area in the continental U.S. with the highest rain load hazard is the Southeast (Louisiana to North Carolina) with average rain hazards ranging from approximately 6.6 to 8.2 inches/hour (16.764 - 20.828 cm/hour) (O'Rourke and Longabard, 2019).

Considerations for wind greatly vary with the location. As can be seen in fig. 18, coastal regions are more prone to higher wind speed. The map provided by the NGMA can be used to determine basic wind speeds.

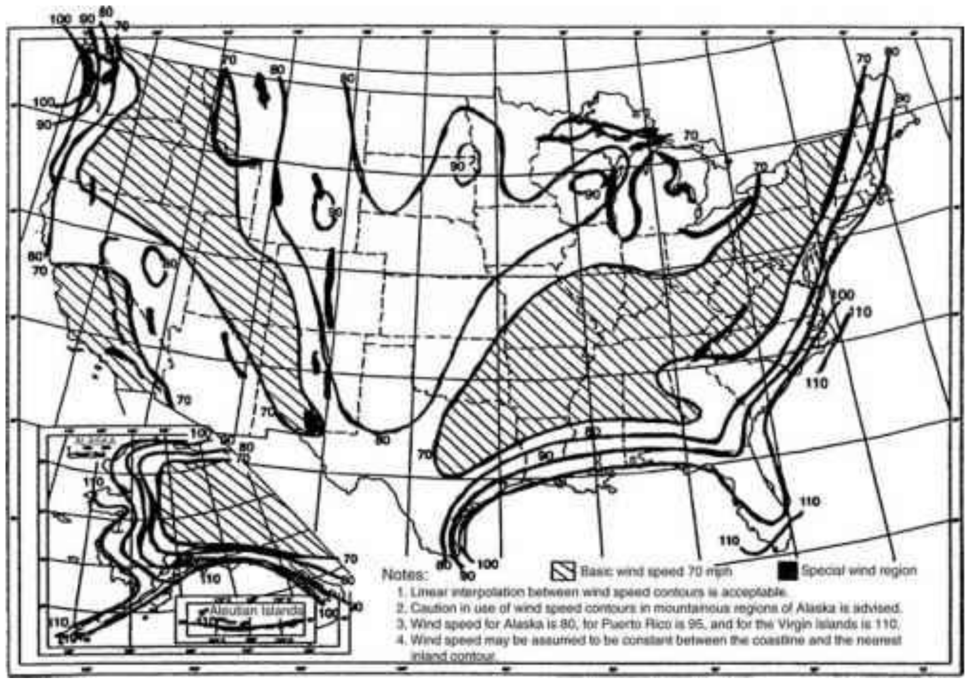

Fig. 18: Minimum basic wind speeds in miles per hour.

The indications on snow loads are different depending on the state (USDA Forest Services, 2013). The team first decided to neglect snow loads. However, the recent climatic events that occurred in Texas especially motivated the team to consider the US historical snow loads, as can be seen on fig.19:

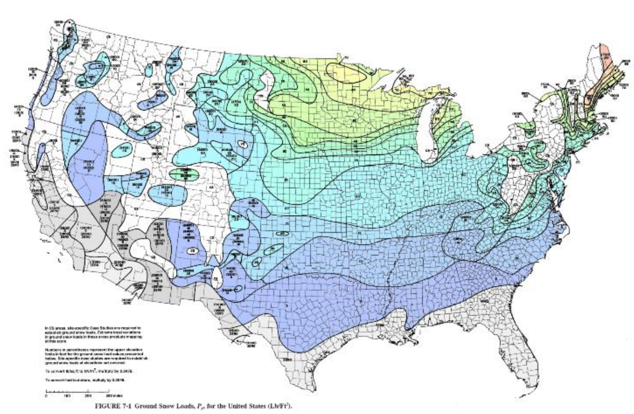

Fig. 19: Ground snow loads, pg, for the contiguous United States (ASCE 7-10 (Figure 7-1), 2016)

As can be seen, values are distributed in the South US from 0 to 25 lb/ft^2

Now that climatic data is gathered, the structural analysis of the prototype will be carried. Then, the theoretical design loads of a commercial structure will be presented, with integration of the prototype additional design components.

5.1.2 Structural Analysis - Prototype

The goal of the analysis is to prove that the system described in this project can be implemented safely to greenhouse structures in the south-US /Northern Mexico. Through its operations, the greenhouse should withstand the minimum weight associated with the diverse types of loads defined earlier. For the autonomous opening/closing mechanism, this means that a Statics analysis should be conducted at two distinct positions. These positions must be completely closed and open, with the load of the cover on top in the second case.

However, it was observed that the structure of the prototype itself would not be able to hold the assembly, thus the team anchored the structure to the roof. In normal conditions, a stronger arched greenhouse structure would have been required. Increasing the height and global dimensions could have been an ameliorating factor too but would have raised the cost of construction significantly.

5.1.4. Design Loads - Commercial Scale

Based on NGMA recommendations for commercial greenhouse, and information from Minimum Design Loads for buildings and other structures, ASCE/SEI 7-10 (Structural Engineer Institute), it is possible to estimate the specific loads of the added components on the greenhouse frame.

Specific Dead Loads

The following components apply for dead loads: PE covering, structural material and bracing, roof extensions, motor platforms and associated motors, integrated rolling bars, rollers, and galvanized steel rails.

The weights of the different components are summarized in table. 2. For convenience, motor platforms, support brackets and housing account for 1kg each.
In addition, the greenhouse structure weight was calculated based on the estimation of the weight of the arches and longitudinal structural bars that compose the frame. The extension roof was assumed to be made of galvanized steel.

Components	Weight (kg)
PE plastic cover	171,12
aluminum embedded bars + rollers	95,4

rails and brackets	150
motors + platform + housing	15
extension roof	282.55
greenhouse structure (18 arches + 5 longitudinal)	1120,3
Total Dead loads	1834.37

Table 2: Weights of all greenhouse components: total dead loads

In this total it is important to note that the portion of the weight added by the novel system represents 61% of the total weight exerted on the greenhouse. This could be an issue and it is important to account for the placement of the roof extension as it would represent about 15% of the total load. Structural studies are required. The details of the dead load calculations are given in Appendix IV. The surface area of the greenhouse is estimated to be approximately 545.34 m^2. Accounting only for the vertical components, the average force acting on the structure is 1834.37*9.81/545.34 = 33 N/m^2. Note however that the weight is not evenly distributed over the greenhouse, as can be seen in fig. 20:

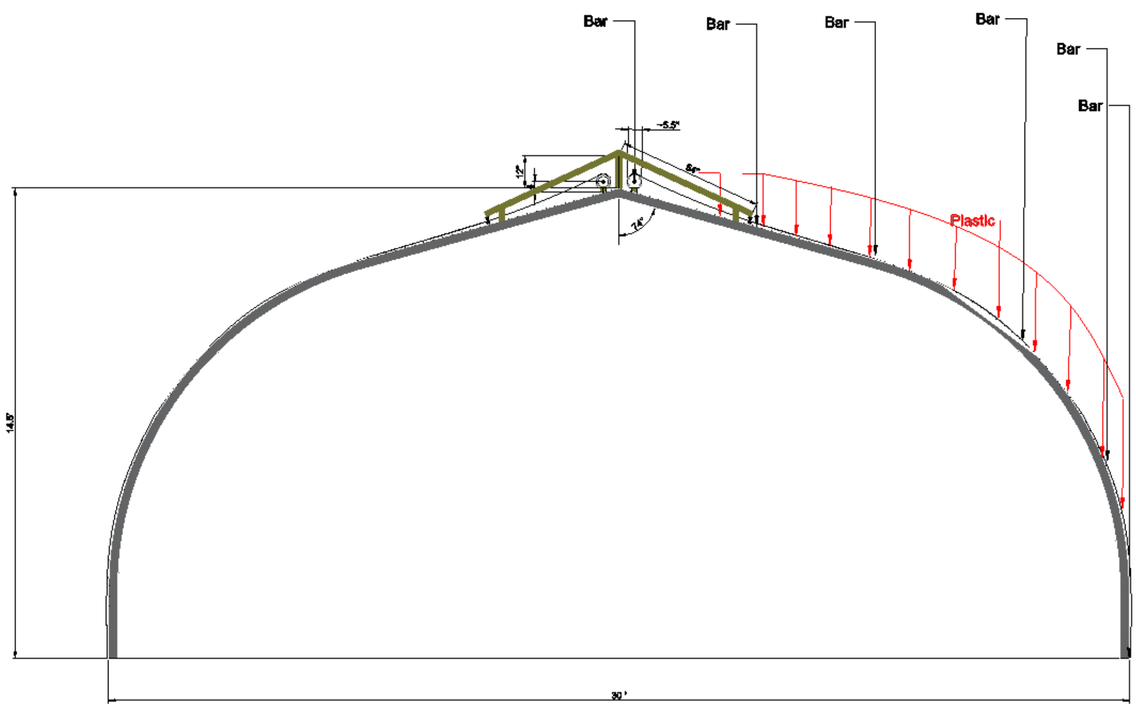

Fig. 20 Load distribution of plastic cover and metal bars when the greenhouse is in closed position.

In this figure, loads associated with the roof extension, and motor assemblies are not shown. It is important to note that the same load is applied on the other side of the greenhouse too. A side view of the greenhouse would have shown that the loads associated with the motors, platform, assembly, and rails are not the same along the greenhouse. Figure 21 is centered on the roof extensions, showing where the load would act when the system is “opened” - or in the upward position.

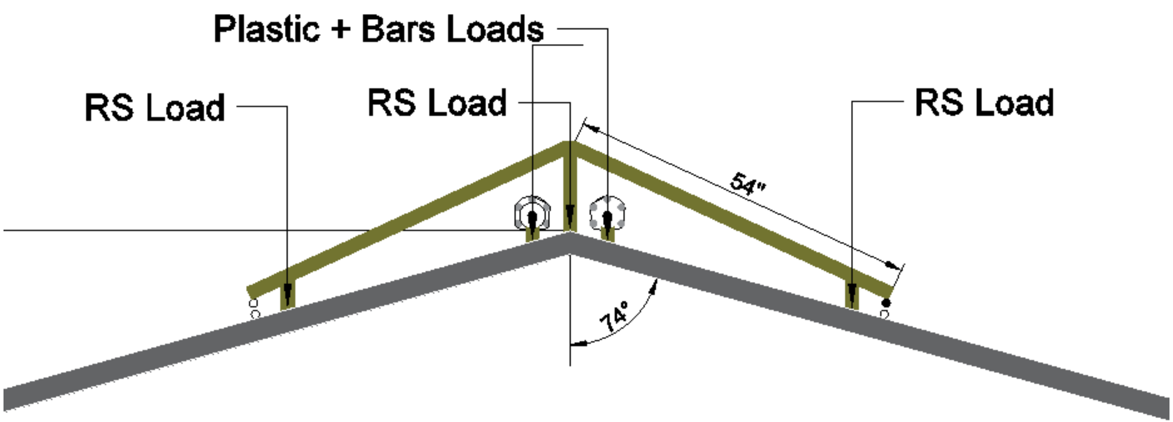

Fig. 21 Load distribution of the Roof structure (RS) and the plastic and aluminum bars when the greenhouse is in open position.

As seen in Figure 21, when the plastic cover is fully rolled up, the load of the roof structure is distributed on 3 main anchoring points on the first and the last arches of each section. As seen in Figure 9, for all the arches in between the firs and the last arches of each section, the roof structure is only attached to the center beam. This therefore means that the dead load of the structure is distributed over 26 load bearing points. A stress analysis of the arch's response to these loads is necessary to determine whether the structure is fit to supper this extra dead load. This analysis will be performed assuming that the weight distribution of the structure is uniform.

Housing dead load stress analysis on galvanised ASTM A-36 steel arches :

$$W = (282.55kg) * (9.81\,m/s^2) = 2.77\,kN$$

Load per leg:

$$Wl = 2.77/26 = 0.107kN$$

The analysis will be performed on the first arch which has three loads acting on it.
As two of the loads are acting at a distance of 13'10" from the footing and the last one is acting at 15', the resultant force acting on the center of the arch can be calculated as such:
13'10" = 13.83"
Resultant force = 0.107 + 2 x 0.107 x 13.83/15 = 0.304 kN acting downward on the tip of the greenhouse's first arch.

Maximum bending moment in the arch:

P: resultant force acting at the ridge
R: radius of the greenhouse arch

$$M = 0.5 * P * R * (1 + cos\theta)$$

$$= 0.5 * 304 * 4.02 * [1 + cos(90)]$$

$$= 611\ N.m$$

Allowable stress :

The American Institute of Steel Construction (AISC) recommends that the maximum bending stress for building-like structures under static loads be kept below $0.66 \times S_y$

The allowable stress is found using both the yield stress of the material (galvanized steel) and the maximum bending stress developed in the arch.

Yield strength of material with integrated safety factor :
S_y = 470 MPa
0.66 Sy = 310 MPa

Maximum Bending Stress:

The polar moment of inertia is found as follows:

$$I = J = \left[\frac{\pi(D^4 - d^4)}{32}\right]$$

In this case, D = 1.25"(3.175 cm) and d = 1.125" (2.85 cm)

So the polar moment of inertia J is 7.914 cm^4 = 7.91
Maximum bending stress is found with:

$$\sigma = \frac{MC}{I}$$

Knowing that

M = 611 N.m
C = the maximum distance from the centroidal axis, in this case it will be the same as the radius of the arches cross section which is equal to 1.25” (0.03175 m)
I = 7.914 cm^4 = 7.91 x 10^{-8} m^4

Maximum Bending stress in the arch:

$$\sigma_{max} = 245.25\ MPa$$

245.25 < 310 MPa, with integrated AISC safety factor.

Therefore, the design is accepted for bending.

Maximum Transverse Shear

Assuming the arches act as a hollow shaped beam, the maximum transverse shear at a critical point is expressed as follows :

$$\tau_{max} = 2V/A$$

Where:
A is the shear Area
V is the force applied on the shear plane
With a shear strength of 400MPa for the chosen material

A= 15.7*0.125 = 1.9625 in^2= 0.001266 m^2
V= 304 N

This yields:

$$\tau_{max} = 2 * \frac{304}{0.001266} = 0.480\, MPa$$

0.480 MPa << 400 MPa , therefore the design is accepted for shear.

Specific Live Loads

Arched greenhouse roofs should be able to support the minimum live load specified in the following equation:

$$L = 20 * R1 * R2 * 12\ (pounds\ per\ square\ foot\ of\ horizontal\ projection)$$

With,

R1 = 1.0	for At < 200
= 1.2 - 0.001*At	for 200 < At < 600
= 0.6	for At > 600

At is the tributary area in square feet supported by the structural member under consideration. The tributary area is a loaded area that contributes to the load on the member supporting that area. It can be tricky to estimate tributary areas for arched greenhouse structures due to their geometry. Tributary area relates to tributary loads, which are found by concentrating the load into the center of the tributary area. The American standard states that all roof members shall be capable of safely supporting a minimum concentrated live load of 100 lbs (45.35 kg) applied downward. In general, the roof extension, arches and longitudinal bars will have the most important tributary areas and will support most of the weight.

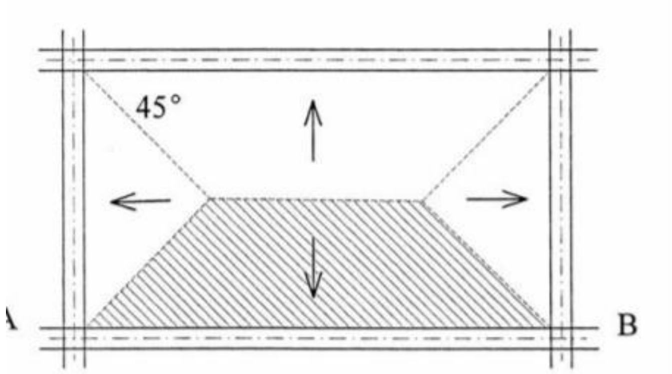

Fig. 22: Repartition of tributary area for two-way structures (Engineering LibreTexts)

As arched greenhouses are curved structures, this estimation will be altered from flat structures. In this theoretical example, the tributary area of the 50 ft arches at the extremities of the greenhouse can be estimated to be the length of the arch times half the distance of spacing in between arches. As 18 arches are used in this theoretical calculations, 100/18 = 5.556 ft spacing is required (1.693 m). The tributary area will thus be 50*5.556/2 = 138.889 ft^2. For an arch in between other arch. The tributary area will be 277.78 ft^2. The tributary area of the 100 ft longitudinal support bars can be estimated with the same methods. There are 5 of these bars in the greenhouse. They have a spacing of 25/3 = 8.333 ft. The tributary area of in between bars would be 100*8.33 ft = 833 ft^2. A better representation of the tributary areas associated a two-way structure is shown below. The theoretical tributary areas for the structural frame of the greenhouse are given in Appendix III.

R2 = 1.0	for F< 4
= 1.2 - 0.05 F	for 4 < F < 12
= 0.6	for F > 12

F is equal to the rise to span ratio multiplied by 32 for an arched roof.
For the following parameters: Rise = 14.5 ft (4.420 m), Span = 30 ft (9.144m)
Thus, F = 14.5/30*32 = 15.5 and therefore, R2 = 0.6.

To account for the tributary space uncertainties, taking R1 = 0.6 to 1.
L = 86.4-144 psf = 4137-6895 N/m^2 of horizontal projection.

In addition, the American Standard for Greenhouse Design states that all components of the structure should be able to withstand 700 N/m^2 live loads on a horizontal projected area. Note that the values found were much higher.

The different load behaviours that could occur on the structure need to be studied. For example, partial load occurring when the whole intensity of the live load is only applied to a portion of a structure / individual member shall be considered to understand the consequences over the entire structure or member. Impact loads should be studied too. Those are often due to rainfall or extreme events which can have multiple undesired effects on the greenhouse (i.e unbalance of the loads, wind speed significant increase). In general, greenhouse suppliers will give information about the acceptable live loads that can act on the structure and need to make sure overloads are not placed on the structure. Live loads related to operation and maintenance (i.e workers fixing/installing the roof extension) and rain loads need to be taken into consideration. Additional precautions should be set regarding rainfalls, such as a water catchment/drainage system for the roof, as accumulated rain on the roof could bring the greenhouse down to failure. In addition, the geometry of a greenhouse is such that other forces will be applied on the structure. A more complete study on the internal stress, bending moments and shear and axial forces will be required with the exact specifications of the greenhouse structure.

Specific Wind Loads

The American Standard set the minimum wind loads that should be supported by greenhouse structural elements at 950 N/m^2 on the vertical projected area. The NGMA provides a whole procedure to determine such loads due to the variability of wind across space and time scales. The procedure is based on the calculations of 3 elements: a velocity pressure (q), a gust response factor (G) and appropriate pressure or force coefficients (Cp and Cpi).

The steps of calculations are summed up in Appendix III. The main-system exposure category D is chosen for the calculation (, for covering material it is always C), relating to an open terrain in flat unobstructed coastal areas directly exposed to wind blowing. In addition, the Importance Coefficient (I) will be taken on a range of 1-1.05 to account for the regions subjected to hurricanes and intense winds (Southeastern US, coastal Mexico) and other Southern US inland regions. The rise of the greenhouse structure of interest in about 12 ft. The velocity exposure coefficient Kz will thus be between 0.8 and 1.2. and the gust response factor between 1.15 and 1.32. The last part consists in choosing external and internal pressure coefficients for the roof and walls. Appendix III gives the tables used to determine these coefficients.

Considering the walls: The values for windward and side walls are given in the previous table. For leeward walls, the value depends on the ratio d/b, namely the horizontal dimension of the greenhouse parallel to wind direction over the horizontal dimension of the greenhouse perpendicular to the wind direction ridge line. For wind blowing in the transverse direction, d/b = 30/100 = 0.33. For wind blowing in the longitudinal direction (along the 100 ft greenhouse), d/b = 100/30 = 3.33. An interpolation was made to find the value in that case. The values –0.5 and –0.233 were finally chosen.

Now, **considering the roof** of an arched greenhouse and assuming that the side walls of the greenhouse are straight on 2.5 feet. The rise-to-span ratio r - defined in fig. H of the Appendix IV - is 12/30 = 0.4 and the greenhouse roof is elevated. For distinct parts of the roof, the external coefficient will be:

Cp (windward quarter) = 2.75*0.4 - 0.7 = 0.4

Cp (leeward quarter) = -0.5

Cp (center half) = -0.7-r = -1.1

Finally, the internal coefficient Cpi is given ranging between –0.25 and 0.25. The maximum wind speeds retrieved from the weather US and Mexican data will be used here and was assessed at a height z = 10m. A value V = 110 mph (177.03 km/hour) is used.

Q(z=h) = 0.00256*K2$*$ (I $*$ V)^2 = $0.00256 * 0.8 * (I * 110)^2$ = [24.7808 ; 27.3208] for exposure C and [37.1712 - 40.9812] for exposure D

For the roof: (*exposure C*)
P(windward) = Qh (G*Cp) - Qh(G*Cpi) = 24.7808*(1.32*0.4) - 24.7808*(1.32*(Cpi) = [4.91 ; **23.44**] psf
P(leeward) = 24.7808 (1.32*-0.5) - 24.7808 (1.32*(Cpi)) = [**-24.53** ; -9.016] psf
P(central half) = 24.7808 (1.32*-1.1) - 24.7808 (1.32*(Cpi)) = [**-44.16** ; -30.65] psf

For the main structure: (*exposure D***)**
P(windward) = Q (G*Cp) - Qh(G*Cpi) = [10.69 ; **35.35** psf] or [511.8; 1692.6 N/ m^2]
P(leeward) = [-11.78 ; **-32.06**] psf --> transverse wind [-564 ; 1535 N/m^2]
P(leeward) = [**-22.76** ; 0.73] psf --> longitudinal wind [-1089.8 ; 34.86 N/m^2]
P(side walls) = [**-44.77** ; - 19.24] psf [-2143.6 ; -921.2 N/m^2]

This is summed up in the following figures, for transverse and longitudinal wind blowing:

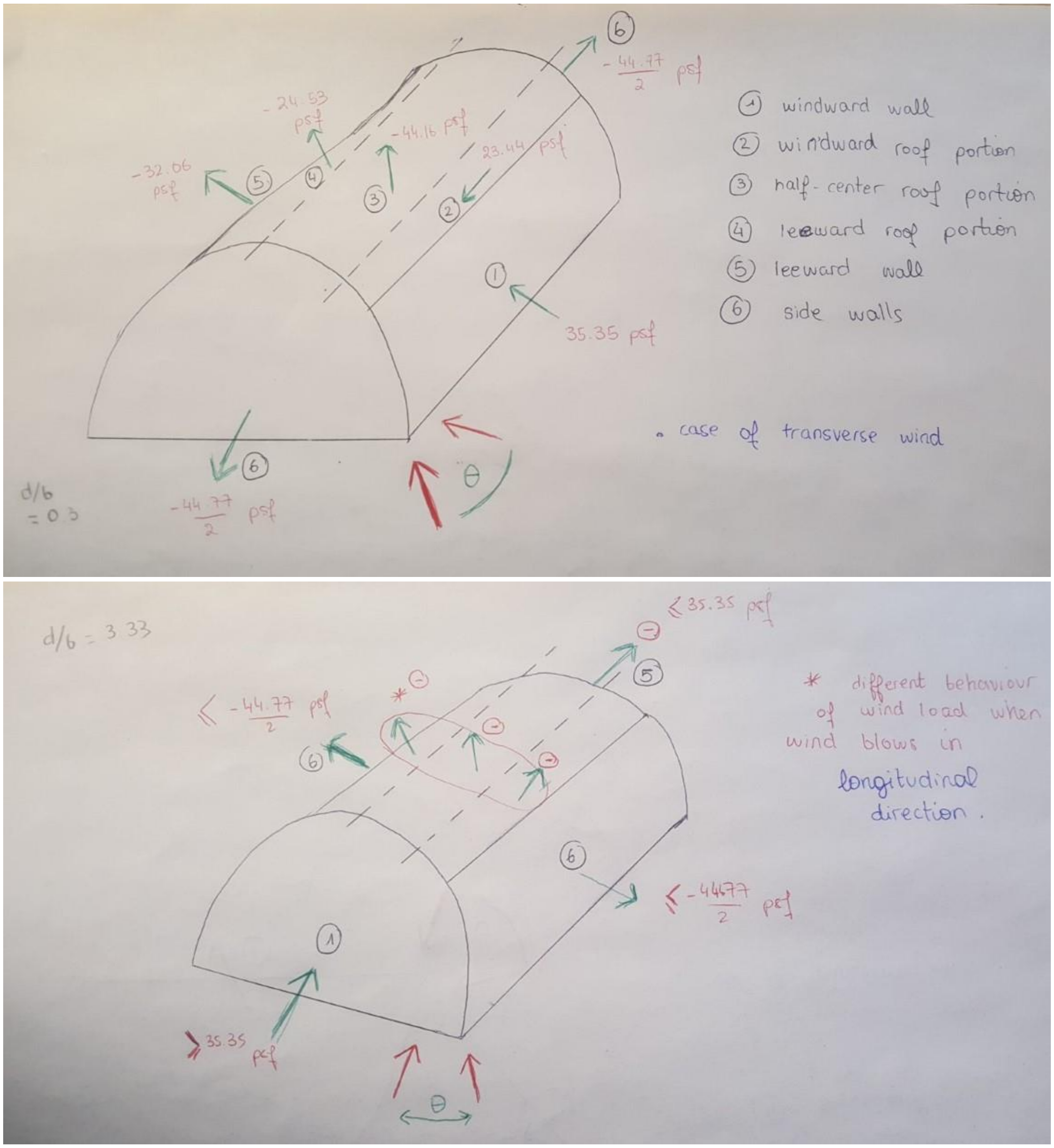

Fig. 23: Estimation of wind pressures on arched greenhouse structure under 110 mph basic wind speed

Even though the calculations were undertaken with several assumptions, from this drawing we can identify and quantify the impact of wind on specific portions of the greenhouse structure. Under transverse high-speed winds, the structure would experience strong outward vertical load on the top of the structure, at the half-center of the roof. This is interesting, since this load could be opposed with the weight of the roof extension, the motor assembly, and rolled-up bars. Caution should be employed when conceiving this part of the system, especially, the weight of the roof extension should not pose failure risks on the greenhouse frame. On the leeward part of the greenhouse, the railing system, with the bars in the PE double layer, should be conceived to be able to sustain this pressure without compromising the integrity of the system. This feature should be ensured even with the mechanism in the opened upward position. The rollers should be inserted in the rails such that the maximum wind pressures don't dislocate them. The interactions between the PE cover and the aluminum embedded bars should also be studied for shear and internal stresses. For further work, design wind simulations and wind-tunnel tests with the design proposed in various positions. The roof extension should also be studied for aerodynamics to assess its behaviour under wind conditions and thus if it is possible to add it to the greenhouse structure. Finally, if it is desired by consumers, the covering should be able to withstand the maximum wind load acting horizontally inside the structure, namely 35.35 psf (1692.56 N/m^2) for 110 mph wind speeds. The maximum vertical wind pressure 44.77 psf (2143.6 N/m^2) going outwards should also be noted as it is important to account for such pressure in regions of high hurricane risks.

Specific Snow Loads

The calculations for snow load vary depending on the local authority and the geographical location. There are usually few snowfalls in the Southern US and North of Mexico. However, due to the mentioned events in Texas, the team decided to make an overestimate, based on the historical snow falls in the region and some assumption. To have satisfactory measures taken for this regard, the maximum ground snowfall value that will be used in the analysis will be pg = 100 psf or 4788 N/m^2 (about the maximum values in the US). This value is also a step closer to the Candian and Alaskan averages.

Arched greenhouses have sloped roof, we can thus estimate the snow loads acting with the following formula:

$$Ps = Cs * Pf \ and \ Pf = 0.7 * Ce * Ct * Is * Pg$$

Ce = Exposure Factor

Ct = Thermal Factor

Is = Importance Factor

Pg = Ground Snow Load (psf)

For a terrain falling in category D, with a fully exposed roof, Ce = 0.8.

The thermal factor will be taken in a range from 0.9 to 1.3, from heated greenhouse to passive greenhouse, as it could yield interesting results. The Importance factor will be assumed 1.

Finally, Pf = 0.7 * 0.8 * Ct * 1 * 100 = [50.4; 72.8] psf

Cs, the roof slope factor, depends on the thermal factor Ct and the angle of curvature of the roof. As can be seen in fig. 20, the roof is curved at an angle of 16°. In addition, the PE cover and galvanized steel roof frame and extensions can be assumed a slippery surface.

With ranging thermal coefficients, this gives 3 different values of Cs. Namely, 0.85, 0.9 and 1 for warm roofs, cold roofs with Ct = 1.1 and cold roof with Ct > 1.2, respectively.

Finally, Ps = [0,85 or 0.9 or 1] * [50.4 ; 72.8] which gives a minimum value of snow loads of 42.84 psf and a maximum value Ps = **72.8** psf (3485.68 N/m^2)

In practice, loads can act in combination (except live and snow loads). We thus must consider cases in which:

- Dead loads act only.
- Dead loads + Live loads act together.
- Dead loads + Live loads + Wind loads act together.
- Dead loads + Snow Loads act together.
- Dead Loads + Snow Loads + Wind Loads act together.

The ASCE 7-10 lists the combination of possible loads and the ratio associated (i.e 1.4 Dead Loads + 0.7 Live Loads). The structure should thus be able to support higher weights than what was calculated. In addition to this, there are multiple ways the loads could behave together. For example, when the loads are unbalanced, additional measures should be taken to avoid stress reversal. Falling of snow should also be monitored for the safety of the people potentially working on and in the greenhouse.
Finally, the mechanical analysis conducted by the team could not be completed more than this due to missing or incomplete information. To be able to provide an acceptable mechanical analysis, more precise data of the structure is required. For the implementation of the design proposed, it will be important to investigate the geometry of structural elements, the distribution of nodes in between structural elements, as well as the greenhouse roof dimensions, and foundations characteristics. The resulting bending moment, internal stresses, shear, and axial forces must be evaluated correctly to ensure acceptable safety levels regarding the structure integrity. The expertise of a structure engineer would be required.

5.3 Safety Standards

For the multistage greenhouse, the following relevant standards are outlined by the Occupational Safety and Health Administration (OSHA):
1910 Subpart J – General Environmental Controls
1910.142, Temporary labor camps

- All sites must be adequately drained and cannot be located within 200 feet of swamps, pools, sink holes, or other surface collections of water.
- The grounds of the greenhouse must also be maintained in a clean and sanitary condition.

1910.145, Specifications for accident prevention signs and tags.

- Hazards due to heat in the components require clear labelling and/or sign postage adjacent to the system.
- Danger due to moving components require warning signs.

1910 Subpart K - Medical and First Aid

- Readily available medical supplies on site

Moreover, given that the main mechanical components of the system are housed at heights exceeding 14 ft, occupational health and safety considerations need to be respected for workers who participate in its installation and/or maintenance. In fact, according to Canadian occupational health and safety standards, if you are at risk for falling three metres (10 feet) or more at your workplace, you should wear the appropriate fall protection equipment.

For information on the procurement, inspection, and installation of safety equipment relevant to working at heights, users should refer to the series of CSA Standards Z259, including:

- Z259.1-05 (R2015) "Body belts and saddles for work positioning and travel restraint",
- Z259.2.3:16 "Descent devices",
- Z259.10-12 (R2016) "Full Body Harnesses",
- Z259.11-17 "Personal energy absorbers and lanyards",
- Z259.12-16 "Connecting components for personal fall-arrest systems (PFAS)",
- Z259.17-16 "Section and use of active fall-protection equipment and systems",
- and any other standards or legislation that may apply.

5.4 Operation and maintenance

5.4.1. Grid costs

To estimate the grid costs of our system, we need to estimate the total power consumption and associated cost for the motors. We can neglect the power consumption from the other small electronic components as they are insignificant compared to the motors.

Motor

The chosen motors have the following electrical properties:

• Recommended Voltage: 12 V DC
• Rated Current: 2.8 A

Therefore, power rating is determined by:

$$P = V * I$$

Yielding:

$$P = 12 * 2.8 = 33.6\,W$$

Thereby, the operation of all motors consumes:

$$Pm(total) = 33.6 * 6\ W = 202\,W$$

As explore in part 4, the operation time to is two minutes to completely open a greenhouse section. Assuming the greenhouse sections each go through two full open and close cycles each day, this means the motors operate for eight minutes total.
Thus, the kwh consumption is calculated as follows:

$$kWh = Watts * \frac{Time(hrs)}{1000}$$

The resulting billable amount is:

$$kWh = 202 * \frac{0.133}{1000} = 0.027\,\frac{kWh}{day} = 9.8\,\frac{kWh}{year}$$

Display screen

Assuming an iPad Pro is used 8 hours a day to display the GUI parameters during a daily work shift, with a power usage of 12 W, the consumption is:

$$kWh = 12 * \frac{8}{1000} = 0.096\,\frac{kWh}{day} = 35\,\frac{kWh}{year}$$

Average residential price of electricity per kWh in Texas as of 2021 is 11.39 cents per kWh, therefore total yearly cost for motors and display is:

$$Price = kWh * 0.1139 = (9.8 + 35) * 0.1139 = 5.1\,USD$$

Therefore, the grid costs for the system amount to 5.1 USD, which is almost negligeable when compared to other associated operation and maintenance costs.

5.4.2. Labor and Repair costs

The costs of running the multistage greenhouse:

- Approximation of 10 minutes per day is spent activating the system through the GUI and supervising the operations.
- Average hourly wage of a Greenhouse Technician is $15 per hour

$$Cost\ (per\ day) = \frac{\$15\ per\ hour}{60\ minutes} * 10\ minutes\ =\ \$2.5\ per\ day$$

$912.5 per year to operate the roll up system.

The cost to repair a greenhouse depends significantly on the nature of the repair, the time, and ease of access and geological location. On average the costs of hiring contractors to repair (including materials) a greenhouse in Southern United States $1475. The most common repair, a broken metal frame can cost approximately $2.50 per linear foot.

Replacement part cost – electronics

Arduino: $30.00

Raspberry Pi: $60.00

Assuming the electronics require replacement every two years due to the hot climate and high humidity within the greenhouse and a major repair of the greenhouse is required every 10 years. The average yearly total cost of operating the multistage greenhouse is **$1110.1.**

6. Proof of concept and Prototyping

This section will assess the process of decisions that led to the construction of the small-scale multistage greenhouse mechanism prototype. The notion of Technology Readiness Levels (TRL) is introduced here to assess the maturity level of the mechanism. In general, technology projects are evaluated against the parameters for each technology level and are assigned a TRL rating from 1 (lowest to 9 (highest) based on the project's deliverables and progress. The TRL scale is shown in fig. 24.

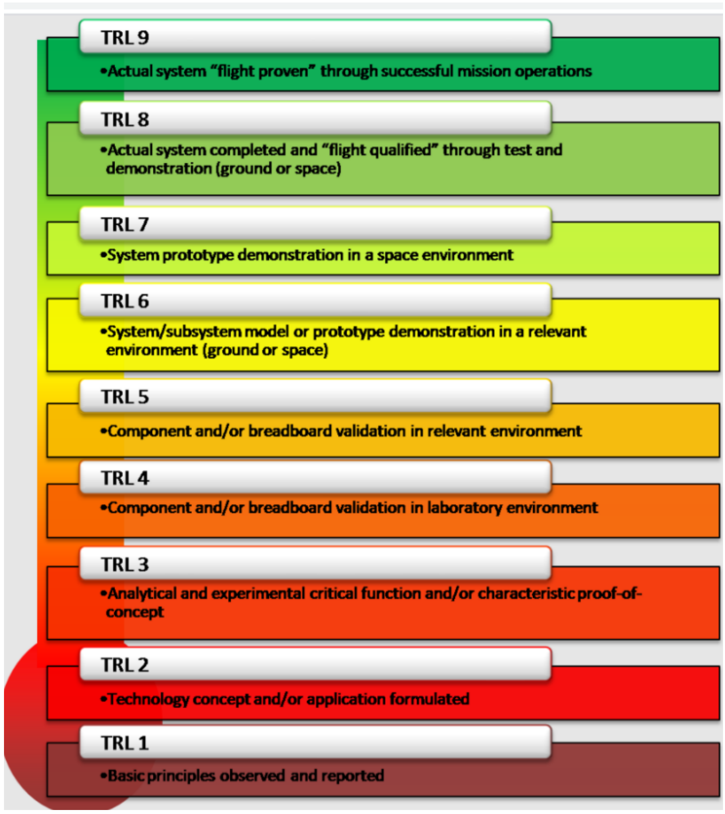

Fig. 24: Technology Readiness Level Scale

Previous work on producing various concept CAD models and a prototype GUI satisfied a TRL 2. The initial idea, given the context and resources available, was to assemble a miniature 3-D printed model with the desired features (C-channel, rollers, small plastic covering, and stepper motor). However, through deliberation, and consultation with our mentor, a proof-of-concept model with TRL 5-6 was determined to be the most suitable.

The prototype implements half of a section of the commercial multistage greenhouse at a smaller scale. The aim of the prototype is to demonstrate a viable proof-of-concept, confirming the automated closing and opening operations of a greenhouse side are possible with a small initial investment. Finally, a prototype of this scale will expose any structural, technological, or ergonomic issues, enabling future review and reiteration of the overall design.

6.1 Materials and Methods

The first consideration that needed to be made when building the prototype was to find appropriate and affordable materials to be used. This section was a specially challenging one since each component of the prototype needed to be fully custom made with a limited budget.

6.1.1 Rollers and Tracks

The polyurethane overhead door rollers are described in Appendix III, with the desired dimensions; a total of 4 rollers were required for the prototype.

For the rail and track system, a review was conducted of all the materials available in nearby hardware stores, it was determined that no match existed for a C-channel track that was wider than 2 inches (to fit the rolling wheels). In addition, no C-channels on the market was able to provide the bending angle required for the system to fit on the greenhouse structure. Therefore, to tackle the problem, the team chose to use acrylonitrile-butadiene-styrene (ABS) tubes that would are bent under the action of mechanical forces (i.e. compressor) and heat (i.e. heat gun). More details are provided in the Prototype Construction section. A total of 2 ABS tubes of 9'½" long and of inner diameter of 2" bought. The properties of ABS are available in Appendix 1.

6.1.2 Structure and Plastic Covering

To construct an adequate yet affordable prototype, the team needed to build the mechanism of interest on a structure that could reproduce the shape of a standard greenhouse. In addition, the structure had to fit within the maximum available height at the construction site.

After some research and careful examination of the construction site, the team decided on buying a 11.5'x10'x7' Walk-in greenhouse structure made by OutSunny, the chosen model was cheap and adapted to the team's specific needs. It also came with a polyethylene meshed covering. The features and specifications of the model are given below.

Fig. 25: OutSunny greenhouse structure fit in the accessible site of construction of the prototype.

Features

- Galvanized steel tube frame with 4 slanted bracing tubes
- UV resistant Polyethylene cover
- Six roll-up windows with mesh protection
- Equipped with 4 pull ropes and 4 ground stakes

Specifications

- Materials: Steel tubes, white Polyethylene cover
- Overall dimension: 11.5'L x 10'W x 7'H
- Window dimension: 1.3′L x 1.3′L
- Door dimension: 4.7'L x 5.7'H
- Accessories: x4 ropes, x4 diagonal braces, x4 ground nails

Modifications

The structure itself was not resilient enough to support the weight of the added ABS rails, metal bars and motor platforms. Therefore, the top section of the greenhouse was hung to the roof and some additional support was brought to the structure during the construction phase.

As mentioned, the specific design of the prototype requires metal bars to be included in the plastic sheet cover. This has the primary goal to enable the upward or downward motion associated with opening and closing the section, respectively. In addition, the bars would ensure tension along the whole polyethylene cover on the length of the greenhouse. The original polyethylene cover sheet was thus slightly modified for the purpose of the project, then the portion of the plastic sheet of interest was cut.

To integrate the galvanized steel bars to the plastic sheet, the team investigated heating the plastic while surrounding the bar, which resulted in failures (too much damage was made to the plastic). It was then decided to incorporate slots made of transparent PVC film to the Polyethylene cover in which the bars would fit. The choice of PVC film was made due to its tensile strength. More details about these modifications are given in the Prototype Construction section.

6.1.3 Motor and Electronic Components

Motor

A Nema 23 standard bipolar stepper motor equipped with a planetary gearbox was selected (see fig C, appendix II.) for the build, with comparable properties to the chosen commercial scale motor. This high torque motor was originally designed for an industrial CNC milling engraving machine and was recalibrated to fit the requirements of our prototype. It was chosen for its high maximum permissible torque of 30 Nm., high holding torque delivered by the transmission, and the high maximum allowable axial and radial loads of the shaft of 100 N and 200 N, respectively. These criteria ensured that the motor would provide adequate torque to leverage the greenhouse section material during and between operation cycles, and that the shaft could provide enough torsional strength to avoid deformation. See appendix II for detailed electrical, transmission and physical specifications.

Microstep Driver

A microstep driver was used to improve resonance, control the stepper motor with higher resolution, and provide smoother motion at low speeds. The FMD2740C model microstep driver was selected (see Appendix II). It is designed for Nema 17 and 23 stepper motors, has a range of 12 to 50 VDC, and a 4 A maximum drive current rating, which accommodated the chosen 2.8A rated motor and the 24V AC to DC converter. The chosen driver has 128 microsteps, allowing the user to further subdivide the motor step angle and increase overall smoothness.

Arduino Uno

An Arduino Uno microcontroller board was connected to a computer which, using the appropriate Arduino code as shown in Appendix II., sent digital control signals to the micro step driver to activate the stepper motor in desired sequence. Specifically, the digital ports of the Arduino Uno were connected to the pulse and direction terminals on the micro step driver, as well as on the ground terminals.

AC to DC converter

An AC to DC converter was integrated into the circuit to convert the 110 VAC wall voltage to 24 VDC, compatible with both the micro step driver and the stepper motor. It operated at 60Hz and could accommodate up to 240 VAC.

6.2 Prototype Modeling

After having chosen the appropriate materials and prior to the building process, a 3D model of the prototype was created for a better overview of the required components. In Figure 26, the designed prototype would only include the features required to test the automated opening and closing system of the greenhouse system. Moreover, due to the lack of budget and available height at the construction site, no shaft/motor housing such as seen on the full-scale design was tested on the prototype. Measures were taken on each of the individual components chosen in the design and the model made on AutoCad was made to scale. This allowed for a good overall visualisation and the model and was therefore a good starting point to the building process and limited the possible errors that could occur during construction.

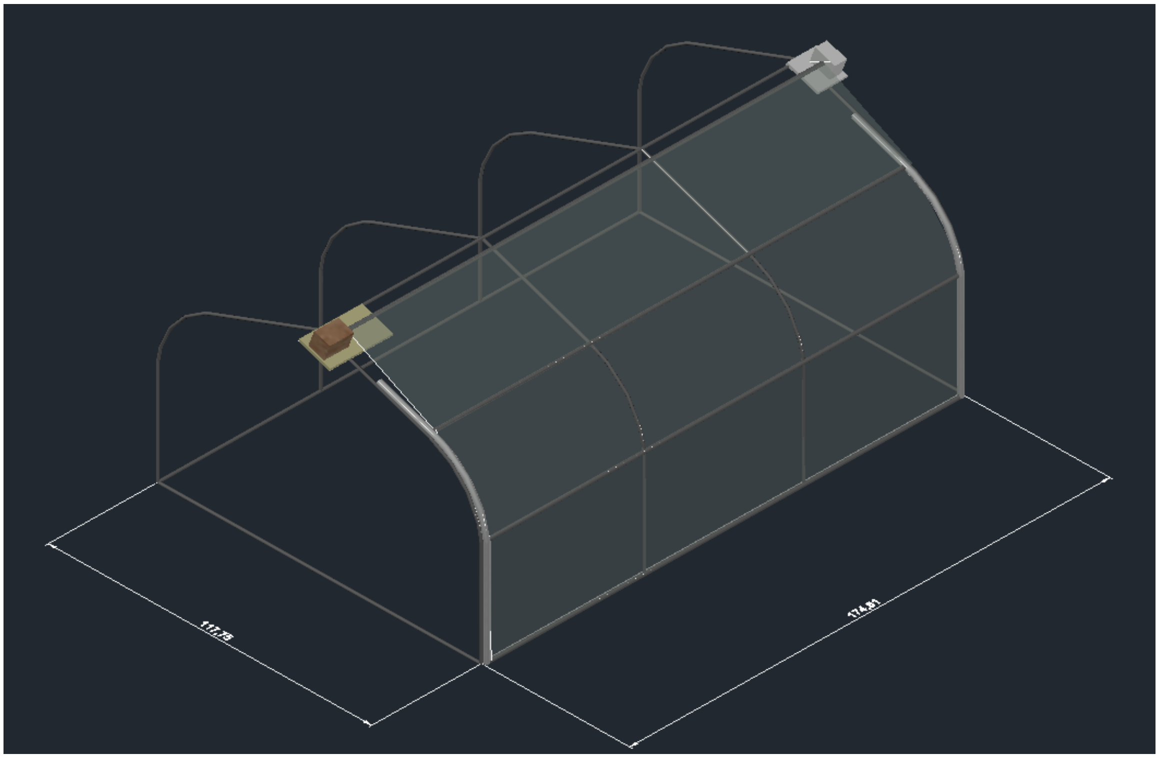

Fig. 26: Prototype AutoCAD 3D model

6.3 Cost of Materials

The final cost of constructing the prototype was $713, Refer to Appendix IV for the summarized Capital expenditure for the prototype.

For comparison, the estimated cost for a full-scale equivalent was 11970.36 $CAD (ref. Report design 2) for 6 independent automatized sections which amounts to around 2000 CAD per section. The prototype was therefore built using ⅓ of the budget of a commercial sized system. Supplementary expenses such as gas and specialized tools were also considered in the prototype cost but were not included in the full-scale estimations.

7. Prototype Construction

7.1 Prototype building process

The construction of the prototype started with a long search to find a suitable location where the prototype could be built inside a building over the course of several weeks to allow the team to start working in the winter and protect workers from the cold, wind, and snow during the building process. A place was finally found on a small farm in Tres-Saint-Redempteur, Québec. In February, the team established a first trip to build the structure of the greenhouse and work on the ABS tubes that were meant to be bended and fitted to the structure as rails.

It took the team 2 to 3 half days to correctly fix the ABS rails to the structure of the greenhouse. The team had to adapt to the situation with the tools available. A grinder and a heat gun were used in addition to mechanical force. Bolts and brackets were even used at strategic points along the PVC and greenhouse structure (see fig. 27) to ensure correct fixation of the new ABS rails.

Fig. 27: Processed ABS tube ready for bending

Fig. 28 Working on the ABS rails

Once the rails were fixed to the structure, more work was needed on the rails (see fig. 28) and more trials were necessary for the team to be able to make the rollers run through correctly. One noticeable challenge was the ABS retraction at the point of curvature of the structure shape (see fig. 29) that would not let enough space for the roller to run through.

Fig. 29: side view of the rail testing with the wheel and steel bar. ABS deformation is noticeable.

After having made sure that the roller movement was satisfying through both sides of the rail mechanism, the team covered the whole structure with the plastic cover and took notes of the dimensions.

In the meanwhile, a platform for the motor was conceived with a portion of rigid High-Density Polyethylene (HDPE). The dimensions of the platform were approximately 50 cm x 40 cm with 0.635 cm thickness.

The motor case and jointure assembly were made with a squared wood box prefabricated. The dimensions are unclear but as shown in fig. 30, the box protects the motor and the stepper motor is linked to the rotating shaft with bolts.

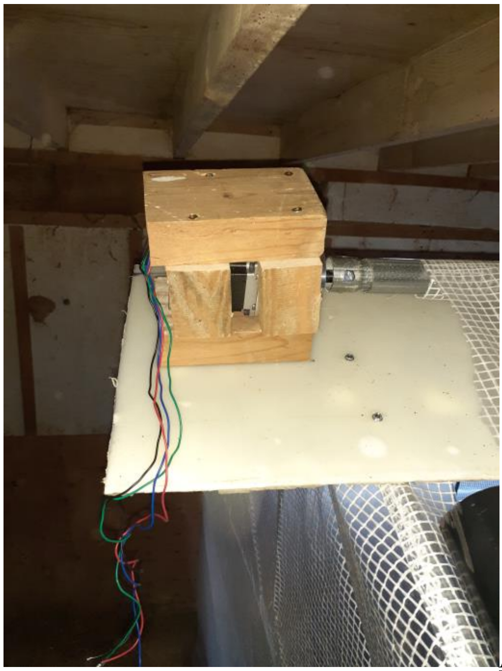

Fig. 30: Motor housing and assembly + platform

The last step before assembling the structure, the plastic opening/closing section and the motor and electronics was to sow the PVC film plastic to the polyethylene cover of the greenhouse. Half of the cover was then cut and brought home for sowing and stapling. The team was able to fit 3 slots along the plastic cover for 3 steel bars to fit in. As a reminder, 2 of these steel bars are integrated with rollers at their extremities to run through the PVC rails.

Fig. 31: Sowing the PVC film slots into the polyethylene cover.

By the end of March, the team was able to correctly integrate the bars to the plastic cover, and the cover over the greenhouse structure, as shown in fig. 32:

Fig. 32: Side and top view of the prototype assembly: ABS rails, polyethylene cover and motor platform

With all the components ready, the prototype was finalized and tested on March 28th. Discussion about the performances of the prototype is undertaken in the next section.

7.2 Automation and Motorization

Automation and motorization on the prototype were designed to replicate the functionality of the commercial scale design. Similar steps were taken as described in Section 4 for the hardware, software, and GUI components. The GUI for the roll up control and automation screen were tested on a 7-inch touchscreen (Figure 33), the large visual cues for the specific roll up section and the control buttons, time selectors, and toggle buttons were easy to operate. However, it was determined that for the commercial-scale system, a larger touchscreen would be more suitable for daily operations.

Figure 33. Graphical User Interface for Roll Up Controls Implemented on a 7” Touchscreen.

8. Discussion on Prototype and Full-Scale Implementation Potential

8.1 Prototype

Once the prototype was built and operational, several tests were conducted to analyse the strengths and weaknesses of the proposed system.

Strengths and Weaknesses

First, it is important to note, once again, that the prototype was built using cheap sub-optimal materials. The fact that the system was able to fully open and stop at the right place while being activated through a GUI clearly demonstrates that the system has some viable potential for commercial applications. Even though the wheels were sometimes catching in the imperfect custom ABS channels, the opening process was shown to be smooth, and a good opening rate was achieved. Using adapted aluminium channels could therefore only better this process. Moreover, as can be seen in figure 34, the prototype confirmed that the metal bars embedded in the plastic could effectively and tightly roll around the top main shaft with no problem. Another detail that the prototype showed is the fact that the friction between the metal bars and the greenhouse arches was negligible and does not produce any unpleasant rubbing sounds. Indeed, as the bars are directly rubbing against the arches while going up, the team though of designing a small plastic cap that could be added to the bar to prevent noises from happening. However, trials showed that the weight of the bars was low enough so that this friction can be assumed to be neglectable.

Fig. 34: Prototype upward position. The metal bars are tightly wrapped around the main shaft.

On the downside, due to time and budget constraints, the rolling down of the greenhouse's side never showed to be working. This is a critical point to contemplate as the going down process is as much important as the going up. After some trials, it was indeed determined that, during the closing process, the wheels were often catching in the ABS rails and stopping the downward motion. This problem could potentially be solved by using well adapted custom rails. Moreover, as the downward motion was only caused by the weight of the metal bars being pulled by gravity, it was determined that at least two bars should not be rolled around the main shaft to keep the roll in tension. A funnel like rail structure is also required to guide the rollers and get them in the tracks. This was confirmed in the trials as the wheels had to be manually guided into the rails. Moreover, as the structure was built in an inside environment, it was not possible to operate the system in windy and rainy conditions to see its behavior. It was observed that the sides of the opening section were not airtight which could be a potential problem if wind gets inside the greenhouse and pushes on the opposite closed panel. Discussions were made on ways to mitigate the air tightness problems and solutions such as adding rubber air sealers on the channels to keep the plastic in the rails were proposed. Trials would be needed to see whether the option is viable.

All of this being said, as the prototype was much smaller in length than a commercial scale greenhouse, those trials are proof that the system would be effective for such a size. It is however a very promising first step in the conceptualisation of such a commercial product and approximations could be made to estimate if the full size could work. In addition, the system shows that sides of a greenhouse cover can be moved with a simple system of tracks and rollers. Therefore, with some efforts and adaptation, implementing a manual version of this system could be feasible in countries with missing or poor electrical infrastructures.

8.2 Potential for product marketability

After a thorough analysis of the design and the current market, a discussion on the potential marketability of the product follows. If the system allows for a smooth rolling up and down of 6 independent sections of a full-scale commercial greenhouse, as previously proposed, the system would be an interesting option for farmers wishing to acclimatise their seedling before transplanting them outside. Indeed, by promoting the efficiency of transplanting seedlings from greenhouses to the outdoors environments, this system can increase the productivity of both small and large-scale horticultural farms that are starting their seedlings in greenhouses.(Arteca, 2015) Having three different environments, if used correctly, is perfect for a slow and steady production of ready to transplant seedlings. This makes it attractive for small farms operating in steady climate countries such as in the tropics. Opening the greenhouse can also be used in horticulture to regulate humidity levels in humid seasons to reduce fungal infestations of crops. Indeed, fungus are a big concern as they constitute the largest number of plant pathogens and are responsible for a range of serious plant diseases. For example, downy mildew is directly caused by high humidity and is one of the most widespread fungal diseases in tomatoes and other vine type crops (Dal Santo, 2009). In countries like Canada, a potential for governmental help for implementing such a system could also exist to help starting horticultural productions acquire such a system.

As the system does not allow air to be blown between the two polyethylene layers like traditional polyethylene greenhouses, the design does not show to be promising for situations where heating would be necessary. It was observed that the proposed design could be sold as an intermediate design between a high tunnel and a traditional greenhouse. High tunnels systems, which are like greenhouses but opened on both ends and on a portion of their sides, are indeed increasingly more in demand all over the world as a form of season extension technology. The system proposed in this paper would allow cold climate countries to extend their growing seasons and open progressively as the season warms up to provide an appropriate temperature to the crops without the need for expensive and motorised blowers. On hot days, instead of continuously running fans, the greenhouse could be opened to the desired height to reduce the greenhouse effect by the plastic cover. This could therefore potentially reduce the electricity requirements and allow for cost savings. In some situations, the multistage greenhouse acclimatization system could be a better option than purchasing a greenhouse or a high tunnel. It indeed provides better heat retention properties than a high tunnel and better airflows than both greenhouses and high tunnels.

Finally, even though the potentials are great and promising, the costs of installation of such a system are estimated to be around 12 000$ for a standard 30* 102’ greenhouse. As these costs are non-negligible, the potential advantages need to provide enough economic benefits to outweigh those initial spending. It is hard to predict the economic benefits associated with better crops performances associated with plant acclimatisation and better temperature and RH control as little research and data has been gathered on these topics. It would therefore be difficult to estimate the potential payback period of such a design without further research and experimentation.

9. Conclusion

Overall, throughout the courses of design 2 and 3, the team designed and elaborated a viable solution to better greenhouse climate control and plant acclimatization processes. After a thorough examination of the customer’s needs and discussions with industry workers, the team focused on an add-on design allowing the automated opening and closing of 6 independent sections to be implemented on a standard 102’ x 30’ gothic greenhouse. In this report, the team specifies the components and mechanisms in use for the project. To better understand the impacts associated with the implementation of such a design on a standard greenhouse, structural analyses of the structure and the major components were performed according to standards. Operation and maintenance, occupational safety and an environmental impact assessment were all made to understand better the implications related to the commercialisation of such a system. Furthermore, to test the feasibility of the design and highlight the potential flaws, a scaled down prototype of a single greenhouse section was built, and tests were performed. The prototype ended up showing a well-controlled and smooth opening of the side plastic, however due to budgetary constraints which led to sub-optimal material usage, the downward motion showed some problems and did not end up working as expected. Solutions were proposed to tackle this problem and more testing using better materials and extra components would be required to verify the viability of the solutions.

Ultimately, after some market analysis it was determined that the proposed design shows some very promising potential for marketability. Indeed, as the proposed solution does not allow for air insulation between the two layers of polyethylene , such a system could find a place on the market as an intermediate between a high tunnel and a traditional greenhouse. As the system would require a non neglectable initial monetary investment, some cost benefits analysis on the increased productivity of crops grown using the system would be necessary to estimate if such an investment is beneficial.

References

Acarnley, P. Stepping Motors: A Guide to Modern Theory and Practice, London, U.K.:The Institution of Engineering and Technology, 2002.

Alexander, T. 2019. Greenhouse Roll up Sides - Benefits, Hardware, Installation. Tunnel Vision House LLC, online website. Accessed November 2020, from: https://www.tunnelvisionhoops.com/bloggreenhouse-roll-up-sides-benefits-hardware-installation/#:~:text=The%20roll-up%20side%20requires%20a%20roll%20bar%20to,extends%20slightly%20past%20both%20ends%20of%20your%20structure.

AlMa'adeed, Mariam. (2015). Processing and characterization of polyethylene-based composites. 10.1179/2055035915Y.0000000002. (density article)

AMCI. N/A. How to Size a Motor. Advanced Micro Controls, Inc. Accessed November 2020, from: https://www.amci.com/industrial-automation-resources/plc-automation-tutorials/how-size-motor/

AMES. 2013. C-CHANNEL SIZES CHART FOR STEEL CHANNELS. Advanced Mechanical Engineering Solutions online website. Accessed November 2020, from: https://amesweb.info/Profiles/Steel-C-Channel-Sizes.aspx

Anaheim Automation, Inc. 2020. Selecting a Stepper Motor System. Accessed November 2020, from: https://www.anaheimautomation.com/manuals/forms/Selecting%20a%20Stepper%20Motor%20System.php

Anthony Petrecca. 1993. Metal Track System for Metal Studs. USOO5222335A. Accessed November 2020, from: https://patents.google.com/patent/US5222335A/en

Arduino. 2020. Arduino Glossary. Accessed November 2020, from: https://www.arduino.cc/glossary/en/

Arteca, R. N. (2015). The Horticultural industry. In *Introduction to horticultural science*. Stamford: Cengage Learning. Accessed from : https://books.google.ca/books?hl=en&lr=&id=3kZvCgAAQBAJ&oi=fnd&pg=PR7&dq=greenhouse+nurseries+horticulture&ots=yHVPiTxmBG&sig=rZl8A3_77SR9k-JX8Sl7s6M0WWY&redir_esc=y#v=onepage&q&f=false on 11/22/2020

Aswinth, R. (2018, October 01). What is Stepper Motor and How it Works. Retrieved November 9, 2020, from https://circuitdigest.com/tutorial/what-is-stepper-motor-and-how-it-works

August, R. 1984. Dynamics of planetary gear trains (Ser. Nasa contractor report, 3793). Lewis Research Center, United States National Aeronautics and Space Administration, Scientific and Technical Information Branch.

Bearings Canada. N/A. Home > Anti-Friction Bearings > Mounted Bearings > 2" Bearing UCF210-32 + Square Flanged Cast Housing Mounted Bearings. Accessed November 2020, from:https://www.bearingscanada.com/2-UCF210-32-Square-Flanged-Cast-Housing-Mounted-p/Kit11952.htm?gclid=Cj0KCQiAzZL-BRDnARIsAPCJs72ZDF858VstEN0e4kJv0eu3DOwUUmNTp1LNFar9u0WDCQhEFmBrxgkaAsflEALw_wcB

Bruhl, D et al. 2020. Benefits of a Stacker Door vs. a Sliding Door. 2020 Home Stratosphere. Accessed November 2020, from: https://www.homestratosphere.com/stacker-door-vs-sliding-door/#:~:text=Sliding%20doors%20are%20the%20most%20commonly%20used%20type,whilst%20the%20fixed%20panel%20doesn%E2%80%99t%20move%20at%20all.

Clarkwestern Dietrich Building Systems LLC. 2020. Structural Tracks. ClarkDietrich online website. Accessed November 2020, from: https://www.clarkdietrich.com/products/curtain-wall-and-load-bearing-framing/structural-track

Consigneco ,Government of Quebec, 2020 *Your cans and bottles have value. Return them.* Accessed on 12/01/2020 form : https://consigneco.org/en/#:~:text=Quebec%20is%20a%20pioneer%20of,processed%20and%20returned%20to%20shelves.

Dal Santo and Holding. 2009, *Best Practice – Downy Mildew in Vegetables*, Accessed on 11/30/2020 from https://ausveg.com.au/infoveg/infoveg-search/best-practice-downy-mildew-in-vegetables/

DOI: 10.17660/ActaHortic.2007.748.27 Accessed from https://doi.org/10.17660/ActaHortic.2007.748.27 on 11/30/2020

Eglowstein, H. (2020, January 10). Introduction to Servo Motors. Retrieved November 10, 2020,from https://www.sciencebuddies.org/science-fair-projects/references/introduction-to-servo-motors

Engineering ToolBox. (2004). *IEC - NEMA Standard Torques*. Accessed November 2020, from: https://www.engineeringtoolbox.com/iec-nema-standards-torques-d_741.html

Franklin Associates. 2020. Cradle-To-Gate Life Cycle Analysis Of Linear Low-Density Polyethylene (LLDPE) Resin. Accessed November 2020, from: https://plastics.americanchemistry.com/Final-ACC-LCA-Report-LLDPE-Resin.pdf?fbclid=IwAR3fwWoJpuEx_BJVbtNYZVVaNKssAbx5B8wKo3f1V5iu_ws1IKRRtkm3G_8

Gay, Warren. (2014). Stepper Motor. 10.1007/978-1-4842-0181-7_27.

Gesellschaft für Bergbau, 2006 Metallurgie, *Rohstoff – und Umwelttechnik*, *Germany* Accessed on 12/01/2020 from https://www.galvanizing.org.uk/sustainable-construction/galvanizing-is-sustainable/recycling/

Gleich, A. 2012. Multi-function roller shutters for roof windows of building. DE102012021737A1. Accessed November 2020, from: https://patents.google.com/patent/DE102012021737A1/en?q=roller+shutters&q=E06B9%2f8

Hameyer, K and Belmans, R.J.M. "Permanent magnet excited brushed DC motors," in *IEEE Transactions on Industrial Electronics*, vol. 43, no. 2, pp. 247-255, April 1996, doi: 10.1109/41.491348.

Harnois Industries. 2017. Product Catalogue. Accessed November 2020, from : https://www.harnois.com/wp-content/uploads/2018/04/Catalogue_Anglais.pdf

Hazarika, B. (2003). Acclimatization of tissue-cultured plants. *Current Science*, *85*(12), 1704-1712. Accessed from http://www.jstor.org/stable/24109975 on 11/29/2020

Helms, M.M. and Nixon, J. 2010. Exploring SWOT analysis – where are we now? A review of academic research from the last decade. *Journal of Strategy and Management*. (3), 215-251. Accessed November 2020, from: https://doi.org/10.1108/17554251011064837

Imhoff, J.C.; Kindig, D.L. 1999. Roll-up doors and curtains. US6155326A

Interview with Mr. André Poulette, Lead Greenhouse Construction and Coach, Les Industries Harnois, Montréal, Canada.

Jacobs, K. 2006. Double side sliding door assembly. US7021007B2 . Home Decor Holding Company, Charlotte, NC, US. Accessed November 2020, from:https://patents.google.com/patent/US7021007B2/en?q=track+and+roller+mechanism&oq=track+and+roller+mechanism

Johnson Bros. Metal Forming Co. N/A. C-channels and box-channels. Products and Services - Online Website. Accessed November 2020, from: https://www.johnsonrollforming.com/display.php/display/A2/category/3

Johnson Bros. Metal Forming Co. N/A. Standard Sizes Chart - C-Channel, Box-Channel, Rectangular & Square Open Seam Tubing. Products and Services - Online Website.

Accessed November 2020, from: https://www.johnsonrollforming.com/pdf/rect_tubing_chart.pdf

Joyce G. Latimer, Tomio Johjima, Kazuyuki Harada,*The effect of mechanical stress on transplant growth and subsequent yield of four cultivars of cucumber*,Scientia Horticulturae,Volume 47, Issues 3–4,1991,Pages 221-230,ISSN 0304-4238, https://doi.org/10.1016/0304-4238(91)90005-J. Accessed from : http://www.sciencedirect.com/science/article/pii/030442389190005J on 11/17/1996

Juneja, P.(N/A). What is Analytical Hierarchy Process (AHP) and How to Use it. Management Study Guide Content Team. Accessed November 2020, from: https://www.managementstudyguide.com/analytical-hierarchy-process.htm

Kenjo, T and Sugawara, A. Stepping Motors and Microprocessor Control, 2nd ed., ISBN:0-19-859385-6, Oxford: Clarendon Press, 2003.

Kraus, T.J. 1989. Roll-up door. US4887660A. Rite Hite Holding Corp. Accessed November 2020, from: https://patents.google.com/patent/US4887660A/en?q=roller+shutters&oq=roller+shutters

Mc-Master Carr. 2020. Corrosion-Resistant 3003 Aluminum Tubes. Accessed November 2020, from: https://www.mcmaster.com/hollow-bars/corrosion-resistant-3003-aluminum-tubes-7/

Mc-Master Carr. 2020. Curved Roller Track for Doors, Curtains, and Strip Doors. Accessed November 2020, from: https://www.mcmaster.com/trolley-roller-track-systems/curved-roller-track-for-doors-curtains-and-strip-doors/

Mc-Master Carr. 2020. Overhead Door Rollers. Online website. Accessed November 2020, from: https://www.mcmaster.com/roller-tracks/overhead-door-rollers/

MRR , Marijuana Retail Report,Wholesale Cannabis Price Index For The Week Ending On March 20th 2020, Accesses from https://marijuanaretailreport.com/wholesale-cannabis-price-index-for-the-week-ending-on-march-20th/ on 11/29/2020

Nor, M.; Rizal & Jalaldeen, M & Razi, M.J.M. & Zakaria, Adlan & Safiuddin, Ahmad & Fakhri, Ahmad & Zulaiha, Puteri & Saat, Abdul. (2018). Cloudemy: Step into the Cloud.

Oltahfer, J.; et al. 1994. Roller door apparatus. US5353859A. Rite Hite Holding Corp. Accessed November 2020, from: https://patents.google.com/patent/US5353859A/en?q=roller+shutters&oq=roller+shutters

Philo, A. (2012, April). HOW TO REDUCE TRANSPLANT SHOCK ON YOUR FARM. *Acres U.S.A. Magazine*. Accessed from https://www.ecofarmingdaily.com/grow-crops/reducing-transplant-shock/ on 11/30/2020

Pyrtek, P. 2017. Roller Mechanism. WO 2017/014650 Al. World Intellectual Property Organization International Bureau. Accessed November 2020, from:https://patents.google.com/patent/WO2017014650A1/fr?oq=International+Publication+Date+WO+2017%2f014650+Al

Quinones, J.I. 2012. Applying acceleration and deceleration profiles to bipolar stepper motors. Texas Instruments Incorporated. Accessed November 2020, from: https://www.ti.com/lit/an/slyt482/slyt482.pdf

Sawicz, D. 2012. Hobby Servo Fundamentals. University of Princeton. Accessed November 2020, from: http://www.princeton.edu/~mae412/TEXT/NTRAK2002/292-302.pdf

Servo Motors. (2020). Retrieved November 15, 2020, from https://www.jameco.com/jameco/workshop/howitworks/how-servo-motors-work.html

Sonkar, A. (2019, January 29). Three simple rules of good touch design. Retrieved December 01, 2020, from https://uxdesign.cc/three-simple-rules-of-good-touch-design-4590e0dd1979

Stoltenberg, K. 2004. Power operated multi-paneled garage door opening system*: US 6719033 B2.* United States Patent. Accessed November 2020, from: https://patents.google.com/patent/US6719033B2/en?q=garage+door+rolling+mechanism&oq=garage+door+rolling+mechanism

Stoneham, J. and Thoday, P. 1985. Some physiological stresses associated with tree transplanting. Scientific Horticulture. 36: 83–91. Accessed on 01/30/2020

Suh, S., Kang, S., Chung, D., & Stroud, I. (2008). Theory and design of CNC systems. London: Springer.

Swiss Bell Farms Inc. Accessed November 2020, from: https://patents.google.com/patent/US6155326A/en

Tang, J. 2020. Motor Sizing Basics Part 2: Load Inertia. Oriental Motor USA Corp. Accessed November 2020, from: https://blog.orientalmotor.com/motor-sizing-basics-part-2-load-inertia#:~:text=Load%20inertia%2C%20or%20moment%20of,referred%20to%20as%20%22J%22.

Teixeira da Silva, J.A., Norikane, A. and Tanaka, M. (2007). *CYMBIDIUM*: SUCCESSFUL IN VITRO GROWTH AND SUBSEQUENT ACCLIMATIZATION. Acta Hortic. 748, 207-213

The Stepper Motor Basics: Types, Working Operation and Applications. (2020, May 15). Retrieved November 8, 2020, from https://www.elprocus.com/stepper-motor-types-advantages-applications/

Türk, Ahmet & Gunal, Efnan & Gurel, Ugur. (2015). An Automation System Design for Greenhouses by Using DIY platforms.

Ulti Group Ltd. 2018. Products - High Speed Doors. Online website. Accessed November 2020, from: https://ultigroup.co.nz/ulti-product/full-vision-doors/

Wang, Y., Liu, B., Ren, T., Li, X., Cong, R., Zhang, M., Yousaf, M. and Lu, J. (2014), Establishment Method Affects Oilseed Rape Yield and the Response to Nitrogen Fertilizer. Agronomy Journal, 106: 131-142. https://doi.org/10.2134/agronj2013.0374 on 11/26/2020

Pierce, D. W., et al. 2014. Statistical Downscaling Using Localized Constructed Analogs (LOCA). Journal of Hydrometeorology, volume 15, page 2558-2585. Retrieved March 2021, from: https://www.climate.gov/maps-data/data-snapshots/data-source-ave-max-temp-high-emissions

NOAA. 2021. State of the Climate: Global Climate Report for Annual 2020. National Centers for Environmental Information. Retrieved on April 11, 2021 from https://www.ncdc.noaa.gov/sotc/global/202013

Burt, C. C. 2019. A Summary of U.S. State Historical Precipitation Extremes. Weather Underground online website. Retrieved March 2021, from: https://www.wunderground.com/cat6/Summary-US-State-Historical-Precipitation-Extremes

Roberts, B, J. 2017. Wind Ressource of the US, Mexico and Central America. Annual average wind speed at 10m above surface level. NREL. Retrived March 2021, from: https://www.nrel.gov/gis/wind.html

https://www.ncdc.noaa.gov/temp-and-precip/us-maps/ytd/202006?products[]=tmax#us-maps-select

USDA Forest Service. 2013. Snow Load Information. Retrieved March 2021, from: https://www.fs.fed.us/eng/snow_load/states.htm

ASCE 7. 2016. Ground Snow Loads for the United States. Chapter 10. Medeek Design Inc. online website. Retrieved March 2021, from: http://design.medeek.com/resources/images/ASCE7-10_FIG7-1_COLOR.jpg

Ponce, P. et al. 2015. Greenhouse design and control. CRC Press, Taylor and Francis Group. ISBN: 978-1-315-77155-7

O'Rourke, M and Longabard, A. 2019. Do structural Engineers design for rain loads? Structural Practices. Retrieved March 2021, from: https://www.structuremag.org/wp-content/uploads/2019/03/261904-C-StructuralPractices-Orourke.pdf

Occupational Safety and Health Administration. (1910). Occupational safety and health standards: Occupational health and environmental control (Standard No. 1910.151). Retrieved from https://www.osha.gov/laws-regs/regulations/standardnumber/1910/1910.151

Occupational Safety and Health Administration. (1910). Occupational safety and health standards: Occupational health and environmental control (Standard No. 1910.142). Retrieved from https://www.osha.gov/laws-regs/regulations/standardnumber/1910/1910.142

Occupational Safety and Health Administration. (1910). Occupational safety and health standards: Occupational health and environmental control (Standard No. 1910.145). Retrieved from https://www.osha.gov/laws-regs/regulations/standardnumber/1910/1910.145

Structural Engineer Insitute. Minimum Design Loads for buildings and other structures, ASCE/SEI 7-10. Retrieved February 2021, from: https://www.waterboards.ca.gov/waterrights/water_issues/programs/bay_delta/california_waterfix/exhibits/docs/dd_jardins/DDJ-148%20ASCE%207-10.pdf

2021 electricity rates by STATE. (2021). Retrieved April , 2021, from https://paylesspower.com/blog/electric-rates-by-state/

Government of Canada – Canadian Centre for Occupational Health and Safety (2021). Body belts, harnesses, And lanyards: OSH answers. Retrieved April 2021, from https://www.ccohs.ca/oshanswers/prevention/ppe/belts.html

APPENDICES

APPENDIX I

Here is shown the initial material list and pricing analysis conducted by the team (total cost is on next page):

Table 1: Cost estimation of commercial scale multistage automated system

Project Category	Product	Quantity /Section	Total Quantity	Pricing / Unit	Total Price	Source
Dome / Plastic	12' x1 1/4" Steel Shafts (1/16)	3	18	28,5	513	Acier Lachine
	Polyethylene Rolls (UV Treated 7.2 mil)(Outside)	N/A	1	5.67$/pi	608	Harnois
	Polythene Rolls (Condensation Treated 7.2 mil) (Inside)	N/A	1	6.6$/pi	707	Harnois
	Arch Adaptors (Custom)	N/A	54	4	216	Lachine
	1ft Dome Support Pipes (1" Square)	6	36	2.8$/20 pi	110	Lachine
	Lock Systems	1	6	20	120	Harnois
	1" Aluminum Plastic Holder Shaft (33') (Emboufte)	6	36	22$/20'	1307	Lachine
Top Shafts	Electric Motors with Gear Box	1	6	95	570	RobotShop
	High Quality 2"Bearings with Mounts	1	6	25	150	BearingCanada
	2" Shaft 33' Aluminium	1	6	80/20 pi	800	Lachine
Rails	25' Roller Tracks	2	12	430	5160	Mc-Master Carr.
	Support Brackets	5	30	23,91	717,3	Mc-Master Carr.
	Roller Systems	12	72	5,59	402,48	Mc-Master Carr.
Electrical / Automation	Arduino Uno R3 USB Microcontroller	N/A	1	25,00	25,00	RobotShop
	Raspberry Pi 4B kit	N/A	1	90,00	90,00	CanaKit
	Arduino motor shield (L293D Motor Drive Shield)	N/A	3	2	6,00	AliExpress

	7 in Capacitive Touchscreen Display for Raspberry Pi	N/A	1	43,75	43,75	AliExpress
	Support Brackets	N/A	1	54,87	54,87	AliExpress
	Jumper Wires (Bulk 120pk)	N/A	3	2,52	7,56	AliExpress
	24AWG Wires (55m)	1/2	3	16,80	50,40	AliExpress
Other	Bolts	50	300	0,5	150	Mc-Master Carr.
	Hex Nuts	50	300	0,5	150	Mc-Master Carr.
	Self Tap Screws	20	120	0,1	12	Mc-Master Carr.
TOTAL					11970,36	

Table. 2: Prototype expenses

Expense	Date	Cost ($CAD)	Source
Test ABS pipes and rollers (x2)	20/02/2021	17	Reno Depot
Greenhouse structure	20/02/2021	200	OutSunny
3-D printing material (excluding the PLA)	20/02/2021	50	Robot Shop
Bearings	20/02/2021	31	Amazon
Microstep driver	20/02/2021	40	Amazon
AC/DC power supply	20/02/2021	31	Amazon
Plastic/glue/bits	27/02/2021	30	Home Hardware
2 Rollers + extra (9 in total)	27/02/2021	31	Patrick Morin
ABS tubes (2) + bolts and nuts, bearings, L-brackets	27/02/2021	74	Rona
Stepper Motor	01/03/2021	100	Amazon

2 extra ABS tubes	13/03/2021	23	Home Hardware
more bolts and nuts	27/03/2021	17	Rona
Transportation expenses (gas.)	through the semester	69	
Total		**713**	

Appendix II - Motor Specifications, Electronic Components, and Arduino Code

Electrical Specification

- Motor Type: Bipolar Stepper
- Step Angle: 0.42 deg
- Holding Torque without Gearbox: 1.89Nm(267.65oz.in)
- Rated Current/phase: 2.8A
- Phase Resistance: 1.13ohms
- Voltage: 3.2V
- Inductance: 5.4mH ± 20%(1KHz)

Gearbox Specifications

- Gearbox Type: Planetary
- Gear Ratio: 15.3
- Efficiency: 81%
- Backlash at No-load: <=1.5 deg
- Max. Permissible Torque: 30Nm(4248oz.in)
- Moment Permissible Torque: 50Nm(7080oz.in)
- Shaft Maximum Axial Load: 100N
- Shaft Maximum Radial Load: 200N

Physical Specifications

- Frame Size: 60 x 60mm
- Motor Length: 76mm

- Gearbox Length: 60mm
- Shaft Diameter: Φ12mm
- Shaft Length: 30mm
- Key-way length: 20mm
- Key-way width: 4mm
- Number of Leads: 4
- Lead Length: 500mm
- Weight: 2.0kg

fig a: Nema 23 bipolar stepper motor

fig b: FMD2740C micro step driver

```
#include <SoftwareSerial.h>

//Define stepper motor connections and steps per revolution:
#define dirPin 2
#define stepPin 3
#define stepsPerRevolution 1600

SoftwareSerial sserial(5,6); // receive pin (used), transmit pin (unused)

void setup() {
  Serial.begin(9600); // used for printing to serial monitor of the Arduino IDE
  pinMode(stepPin, OUTPUT);
  pinMode(dirPin, OUTPUT);
  sserial.begin(9600); // used to receive digits from the Java application
  while (!Serial) {
    ; // wait for serial port to connect.
  }
}

void loop() {
  if (Serial.available()) {  // Returns true if there is serial input.
    char ch = Serial.read();
    //Enter 1 to spin motor CW
    if (ch == '1') {
       //Set the spinning direction clockwise:
       digitalWrite(dirPin, HIGH);
      for (int i = 0; i < stepsPerRevolution; i++) {
        digitalWrite(stepPin, HIGH);
        delayMicroseconds(500);
        digitalWrite(stepPin, LOW);
        delayMicroseconds(500);
      }
    }
    //Enter 2 to spin motor CCW
    if (ch == '2') {
      //Set the spinning direction counterclockwise:
      digitalWrite(dirPin, LOW);
      for (int i = 0; i < stepsPerRevolution; i++) {
        digitalWrite(stepPin, HIGH);
        delayMicroseconds(500);
        digitalWrite(stepPin, LOW);
        delayMicroseconds(500);
      }
    }
  }
}
```

Figure c. Snippet of Arduino Code containing stepper and microstep driver controls.

Appendix III- Commercial Scale Motor

Thus, the chosen motor for our application is a NEMA-23 Bipolar Stepper Motor, with the following properties:

Motor properties:

- Step Angle: 0.023°
- Step Accuracy: ± 5 %
- Holding Torque: 240 kg·cm (23.54 N.m)
- Rated Torque: 240 kg·cm (23.54 N.m)
- Maximum Speed (w/Motor Controller): 25 RPM

Electrical properties:

- Recommended Voltage: 12 V DC
- Rated Current: 2.8 A
- Coil Resistance: 900 mΩ
- Phase Inductance: 2.5 mH

Physical properties :

- Mounting Plate Size: NEMA - 23 (standard)
- Weight: 1.5 kg
- Number of Leads: 4
- Wire Length: 300 mm

Appendix IV - Design Loads Calculations

Dead Loads calculations:

Apart from structure weight, all weights are calculated in the Material section. In order to estimate the weight of the structural frame composed of 18 arches and 5 longitudinal bars, the following was executed:

The volume of the arches was calculated as follows : $pi * h * (R^2 - r^2)$
With h= 50 ft, R= 1 inches and r = 1” - 1/8”
This gives V = 0.00374 m^3 for one arch and thus 18*0.00374 = 0.0673 m^3
As the density of galvanized steel can be assumed to be 8030 kg/m^3, the total weight of the arches is 1040 kg
The volume of the longitudinal bars is given with the same formula, and R = 2” , r = 1.9”
This gives a mass of 80.3 kg
Adding all weights together, the total dead loads are 2116.92 kg.
The surface area of the greenhouse is estimated at 5870 ft^2 = 545.34 m^2

Tributary Area

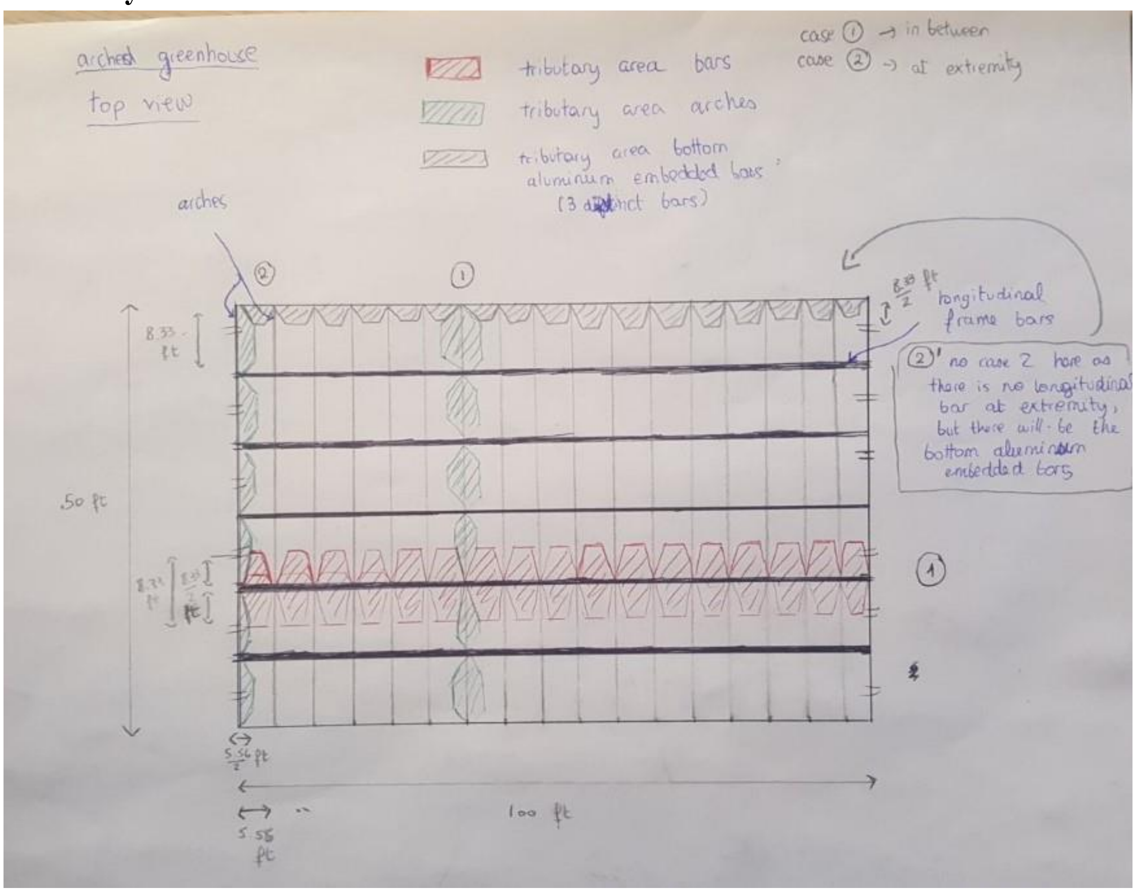

Fig. D: Representation of the tributary areas for each structural element (arch and longitudinal bars)

Wind Loads Calculation information complement:

The equations to estimate the design wind pressure from the mentioned values and coefficients are given in the following figures:

DESIGN WIND PRESSURES (P)

For the main wind-force resisting system:

$$P = qGC_p - q_h (GC_{pi})$$

where:

- q: q_z for windward wall
  q_h for leeward wall and roof
- G: given in Table 5.4
- C_p: given in Table 5.5 and 5.7
- (GC_{pi}): given in Table 5.8

For components and glazing:

$$P = q_h (GC_p) - q_h (GC_{pi})$$

where:

- q_h: evaluated using Exposure C for all terrains
- (GC_p): given in Tables 5.6A, 5.6B and 5.7
- (GC_{pi}): given in Table 5.8

$$q_z = 0.00256\ K_z\ (IV)^2$$

where:

- V: given in Fig. 5.1 in accordance with the provisions of Section 5.3.2
- I: given in Table 5.2
- K_z: given in Table 5.3 in accordance with the provisions of Section 5.3.3

Fig. E: Equations for Design Wind Pressures (NGMA Greenhouse design loads, Chapter 2 and 3)

WALL PRESSURE COEFFICIENTS C_p

SURFACE	d/b	C_p
WINDWARD WALLS	ALL VALUES	0.8
LEEWARD WALLS	0 - 1 2 ≥ 4	-0.5 -0.3 -0.2
SIDE WALLS	ALL VALUES	-0.7

Fig. F: Wall Pressure coefficients

EXTERNAL COEFFICIENTS (C_p) FOR ARCHED ROOFS

Type of Roof	Rise-to-Span Ratio	Windward Quarter	Center Half	Leeward Quarter
Roof on elevated structure	0<r<0.2 0.2≤r<0.3* 0.3≤r≤0.6	-0.9 (1.5r-0.3) (2.75r-0.7)	(-0.7-r) (-0.7-r) (-0.7-r)	-0.5 -0.5 -0.5
Roof springing from ground level	0<r≤0.6	1.4r	(-0.7-r)	-0.5

Fig. G: External coefficients for arched roofs

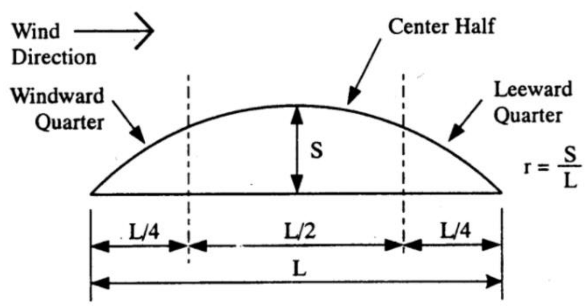

Fig. H: Arched greenhouse geometry for wind loads on roof

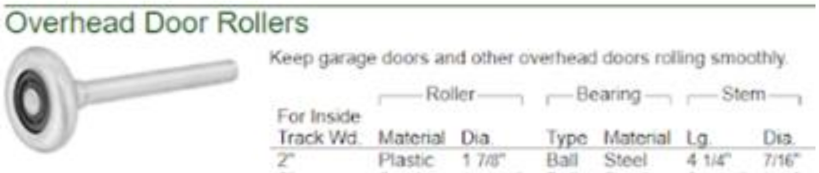

Overhead Door Rollers

Keep garage doors and other overhead doors rolling smoothly.

	Roller		Bearing		Stem	
For Inside Track Wd.	Material	Dia.	Type	Material	Lg.	Dia.
2"	Plastic	1 7/8"	Ball	Steel	4 1/4"	7/16"

Fig. I: Overhead Door Rollers product information (McMaster-Carr, 2020)